MATHEMATICAL MODEL DEVELOPMENT OF THE ANTI TORQUE SYSTEM OF A NOTAR HELICOPTER

A THESIS SUBMITTED TO
THE GRADUATE SCHOOL OF NATURAL AND APPLIED SCIENCES
OF
MIDDLE EAST TECHNICAL UNIVERSITY

BY

HÜSEYİN MURAT BAKIR

IN PARTIAL FULFILLMENT OF THE REQUIREMENTS
FOR
THE DEGREE OF MASTER OF SCIENCE
IN
AEROSPACE ENGINEERING

DECEMBER 2008

Approval of the thesis:

MATHEMATICAL MODEL DEVELOPMENT OF THE ANTI TORQUE SYSTEM OF A NOTAR HELICOPTER

submitted by **HÜSEYİN MURAT BAKIR** in partial fulfillment of the requirements for the degree of
Master of Science in Aerospace Engineering Department, Middle East Technical University by,

Prof. Dr. Canan Özgen _____
Dean, Graduate School of **Natural and Applied Sciences**

Prof. Dr. İsmail H. Tuncer _____
Head of Department, **Aerospace Engineering**

Dr. İlkay Yavrucuk _____
Supervisor, **Aerospace Engineering Dept., METU**

Examining Committee Members:

Prof. Dr. Ozan Tekinalp
Aerospace Engineering Dept., METU _____

Dr. İlkay Yavrucuk
Aerospace Engineering Dept., METU _____

Assist. Prof. Dr. Melin Şahin
Aerospace Engineering Dept., METU _____

Assist. Prof. Dr. Oğuz Uzol
Aerospace Engineering Dept., METU _____

Dr. Nuri Temur
Aviation Dept.,
TURKISH NATIONAL POLICE _____

Date: _____

I hereby declare that all information in this document has been obtained and presented in accordance with academic rules and ethical conduct. I also declare that, as required by these rules and conduct, I have fully cited and referenced all material and results that are not original to this work.

Name, Last Name: HÜSEYİN MURAT BAKIR

Signature :

ABSTRACT

MATHEMATICAL MODEL DEVELOPMENT OF THE ANTI TORQUE SYSTEM OF A NOTAR HELICOPTER

BAKIR, Hüseyin Murat

M.S., Department of Aerospace Engineering

Supervisor : Dr. İlkay Yavrucuk

December 2008, 82 pages

The anti-torque mechanism of a NOTAR helicopter is a complex system including vertical tail and pressurized tail boom which provides air ejection used for both circulation control around the boom and creating directed jet air at the end of the boom. This thesis targets the modeling of this mechanism and integrating it to a helicopter simulation model. Flight tests are performed on the MD 600N helicopter to verify the results. Finally, the simulation is compared with flight test data.

Keywords: NOTAR, helicopter, simulation, modeling

ÖZ

BİR NOTAR HELİKOPTERİNİN ANTİTORK SİSTEMİ İÇİN MATEMATİKSEL MODEL GELİŞTİRİLMESİ

BAKIR, Hüseyin Murat
Yüksek Lisans, Havacılık ve Uzay Mühendisliği Bölümü
Tez Yöneticisi : Dr. İlkay Yavrucuk

Eylül 2008, 82 sayfa

Bir NOTAR helikopterinin anti-tork mekanizması dikey dengeleyici ve basınçlandırılmış kuyruk silindirinden oluşan karmaşık bir sistemdir. Bu sistemde kuyruk silindiri hava çıkışı sağlayarak hem silindirin etrafında sirkülasyon kontrolünü, hem de silindirin sonunda yönlendirilmiş jet akımınının oluşmasını sağlar. Bu tez adı geçen sistemin modellenmesini ve bir helikopter modeline entegrasyonunu hedeflemektedir. MD 600N helikopteriyle yapılan uçuş testleri, sonuçları doğrulamak için kullanılmıştır. Son olarak simulasyon sonuçları uçuş test datası ile karşılaştırılmıştır.

Anahtar Kelimeler: NOTAR, helikopter, simülasyon, modelleme

To my family

ACKNOWLEDGMENTS

I would like to express my gratitude to my supervisor, Dr. İlkay Yavrucuk, whose expertise, understanding, and patience, added considerably to my graduate experience.

I would like to thank to Assist. Prof. Dr. Oğuz Uzol for his advises and interests for this thesis. Thanks to Prof. Dr. Ozan Tekinalp, Assist. Prof. Dr. Melin Şahin and Dr. Nuri Temur for their suggestions.

I wish to state my endless thanks to Deniz Yılmaz, Özlem Ceyhan, Hilal Erçin, Onur Tarımcı and Tahir Turgut for their help and useful discussions.

I appreciate Baki Yıldız, Mehmet Dayıoğlu and also pilots and technicians of TNP Aviation Departmant for helps and supports for the tests. And thanks to Ramazan Yalçınkaya, Beytullah Oğuz, Güntaç Şimşek and İhsan Özge who helped me writing this thesis.

I would like to thank all my friends who helped me get through this thesis.

Special thanks to my fiancee for her endless support, understanding and patience.

Finally, I would like to express my deepest thanks to my parents and my sisters for their infinite support throughout my life.

TABLE OF CONTENTS

LIST OF TABLES

TABLES

LIST OF FIGURES

FIGURES

LIST OF ABBREVIATIONS

ϕ	Roll angle
θ	Pitch angle
ψ	Yaw angle
C_T	Thrust coefficient
ρ	Outside air density
ρ_0	Outside air density
ρ_1	Air density in section 1
ρ_2	Air density in section 2
ρ_3	Air density in section 3
ρ_4	Air density in section 4
ρ_5	Air density in tail boom slots
ρ_6	Air density in section 5
ρ_7	Air density on direct jet thruster
ρ_8	Air density of slot exits
ρ_∞	Air density in main rotor wake
V_a	Axial velocity component at any radial station within fan annulus
V_{θ_s}	Swirl velocity upstream of the stators
V_θ	Vortex flow velocity over circulation control tail boom
V_1	Air velocity on section 3
V_2	Air velocity on upstream of fan
V_3	Air velocity on downstream of fan
V_4	Air velocity on downstream of stators
V_5	Air velocity onside tail boom
V_6	Air velocity on section 6
V_7	Air velocity on direct jet thruster
V_m	Mean air velocity relative to fan blade
V_∞	Air velocity of main rotor wake
A_1	Area of section 1
A_2	Area of section 2
A_3	Area of section 3
A_4	Area of section 4
A_5	Area of section 5
A_6	Area of section 6
A_7	Thruster exit area
A_8	Total area of tail boom slots
p	Body roll rate
q	Body pitch rate
r	Body yaw rate
τ	Pressure coefficient
C_μ	Momentum coefficient
d_s	Tail boom slots height
d_f	Tail boom diameter
d_t	Thruster opening height
Re	Reynold's number
$C_{d,0}$	Drag coefficient of airfoil
C_L	Lift coefficient of horizontal stabilizer
AR	Aspect Ratio
C_D	Drag coefficient of horizontal stabilizer
P_0	Outside air pressure
P_1	Air pressure in section 1
P_2	Air pressure upstream of fan
P_3	Air pressure downstream of fan
P_4	Air pressure downstream of stators
P_5	Air pressure inside the tail boom
P_6	Air pressure in thruster
ΔP_{Tth}	Theoretical total pressure rise
ΔP_{Tf}	Total pressure loss of fan
ΔP_{Ts}	Total pressure loss of stators
T	Thrust
R	Main rotor radius

Z	Altitude of hub
V_f	Forward velocity
V_i	Induced velocity
L	Roll moment
M	Pitch moment
N	Yaw moment
I_X	Inertia in body x-axis
I_Y	Inertia in body y-axis
I_Z	Inertia in body z-axis
I_{XZ}	Inertia on body x-z plane
U	Velocity in body x-axis
V	Velocity in body y-axis
W	Velocity in body z-axis
$\%Pd$	Pilot pedal input
$\%Q$	Engine torque
$\%Cp$	Pilot collective input
g	Gravity of earth
F_x	Force in body x-axis
F_y	Force in body y-axis
F_z	Force in body z-axis
$N_{thruster}$	Yaw moment produced by direct jet thruster
$F_{thruster}$	Side force produced by direct jet thruster
$l_{thruster}$	Moment arm between CG of the helicopter and direct jet thruster
N_{boom}	Yaw moment produced by circulation lift tail boom
$N_{boomhover}$	Yaw moment produced by circulation lift tail boom in hover
$(N_{boom}/N_{boomhover})_{forward}$	Effect of forward flight to yaw moment produce by circulation lift tail boom
$(N_{boom}/N_{boomhover})_{side}$	Effect of side flight to yaw moment produce by circulation lift tail boom
F_{boom}	Side force produced by circulation lift tail boom
l_{boom}	Moment arm between CG of the helicopter and mid section of the circulation lift tail boom
$MDHC$	McDonnel Doglas Helicopters Co's
K	Non dimensional loss coefficient
K_I	Non dimensional loss coefficient of air inlet
K_f	Non dimensional loss coefficient of fan
K_s	Non dimensional loss coefficient of stators
K_d	Non dimensional loss coefficient of diffuser
K_b	Non dimensional loss coefficient of tail boom
K_t	Non dimensional loss coefficient of thruster
f	Friction factor
c_l	Fan blade lift coefficient
C_{D_P}	Profile drag coefficient at mid blade span of the fan
C_{D_S}	The secondary drag coefficient of the fan
ϵ_s	Swirl coefficient on the downstream of fan
m	Fan blade lift curve slope
σ	Fan blade solidity
α	Angle of attack of the fan blades
Ωr	Blade velocity at mid blade span
r	Radius of the fan blade mid span
λ	Flow coefficient
β_m	Angle that V_m makes with fan axis
β_N	Value of β_m for fan no lift condition
F^l	Force production per lenght of the boom
Γ	The strength of circulation lift
ψ	The stream function
κ	Doublet flow strength

CHAPTER 1

INTRODUCTION

The classic tail rotor has been the most commonly used anti-torque mechanism for single main rotor helicopters [1]. Although a simple design it has some disadvantages. One disadvantage is in terms of flight safety. According to U.S. Army safety reports, 20% of all peacetime helicopter accidents are caused by tail rotors [2]. In addition, tail rotors are noisy.

Other anti-torque alternatives to the classic tail rotor have been developed. One is the tip jet rotor, where the main rotor is not driven by the mast, but from nozzles on the tip of the rotor blade; which are either pressurized from a fuselage-mounted gas turbine or have their own turbojet, ramjet or rocket thrusters. Although this method is simple and eliminates torque, it is less fuel efficient than conventional helicopters and produce more noise [2]. Another one is the counter rotating main rotor configuration. In this configuration main rotors are turning in opposite directions to counteract the effects of torque on the aircraft without relying on an anti-torque tail rotor.

An alternative to the classic tail rotor is the No Tail Rotor (NOTAR) concept. The NOTAR helicopters flying today were designed and tested by McDonnel Douglas Helicopters Company (MDHC) [3]. The NOTAR uses the anti-torque by using the Coanda Effect by controlling the circulation on the tail boom and directed jet of air at the aft end of the boom of the helicopter. The use of directed air to provide required anti-torque was used as early as 1945 in the British Cierva W.9 [4] but could not go beyond than an experimental helicopter. On the other hand, the use of circulation control on the tail boom used is as early as in the 1960's. J.G. Lee has invented a helicopter anti-torque mechanism which utilizes a flow of air to create a circulation on the tail boom of the helicopter. But this concept has never been built. The idea of using both circulation control tail boom and direct jet thruster for obtaining anti-torque appeared

in a Lockeed project called ”Advanced Anti-torque Concept”in 1971 [3]. The invention of Lockeed engineer Joe Valazquez is quite similar to today's NOTAR concept. Although the MDHC did not invent the NOTAR concept, the company developed the current state of the art NOTAR anti-torque system. The state of the art NOTAR concept is an anti-torque system, which is composed of an enclosed fan that is driven by the main transmission, a circulation control tail boom, direct-jet thruster and horizontal stabilizer with two vertical stabilizers (H-Tail) [1]. And there are three licensed helicopter is flying today; MD 530N, MD 600N and MD 900.

Mathematical modeling of helicopters for simulations goes back to the 1970's. However, in those years the computing power was not enough and complicated models were not possible to run in real time [5]. Today, both the required computer power is available and aerodynamic modeling is improved making realistic real-time simulations possible. As a result simulated flight became a standard in the industry and a lot of companies prefer simulation since it is cheaper and safer.

Although its wide use for many years no known mathematical model for the NOTAR system has been presented in the open literature yet. Although it is well known conception that the modeling of the NOTAR anti-torque system of a helicopter can be handled through a similitude to a tail rotor, this is not entirely true. NOTAR and Tail Rotor flight characteristics have many differences. For instance the NOTAR anti-torque system would require more control input in general when compared to traditional tail rotor, a well known fact reported by pilots. Similarly the transient performance is significantly different. Therefore, a mathematical NOTAR model would increase the quality of simulations that use the NOTAR concept.

In modeling the NOTAR system the air flow is analyzed by dividing the system into 6 control volumes and specifying 8 sections. The thrust produced by the direct jet thruster and circulation control tail boom is found. For the tail boom calculations some of the flight test data performed by the MDHC is used. Lastly vertical tail effect is added to the model. During the model development the information that the circulation control tail boom provides nearly 60% of the required main rotor anti-torque, and the direct jet thruster produces the remaining in a hover flight is used as stated in [3], [2], [6], [7], [8], [9] and [10]. A major assumption was that the exit velocity of the thruster was constant. It is found that the pressure inside the circulation lift tail boom is constant, stated previously in [3], [8] and [2].

The developed NOTAR anti-torque model is integrated to the minimum complexity helicopter simulation math model program [11]. Firstly, the simulation tail rotor calculations are replaced with the NOTAR model. Then, the vertical tail model is updated. Then, the MD 600N helicopter properties are included to the program. The original computer program was developed using the C++ programming language [12].

The MD 600N helicopter -one of the three certified NOTAR helicopters- is flight tested in order to compare and validate the developed NOTAR model. The helicopter was instrumented and flight tests are performed. The data obtain from the flight tests are analyzed and compared with the simulation model. First the hover and forward flight trim values are compared. Then several different pilot pedal input responses of the model in hover are compared with the MD 600N flight test data. The results showed that the model has promising matched responses with the flight test data.

This thesis is organized as follows: Chapter 2 describes the history, development and principles of the NOTAR anti-torque system. Each component of the system is treated in this chapter. In Chapter 3, the aerodynamic solution of each component and development of the NOTAR anti-torque model are described. Chapter 4 shows the flight tests using the MD 600N helicopter. In Chapter 5 the model is integrated into the minimum complexity helicopter model and is verified with flight test results. Finally, Chapter 6 presents conclusions and recommendations for future work.

CHAPTER 2

NOTAR HISTORY, DEVELOPMENT AND SYSTEM DESCRIPTION

2.1 History and Development

The most common way to produce anti torque is with the use of a tail rotor. The tail rotor is a variable-pitch propeller mounted sideways at the rear of a helicopter. Nonetheless, the tail rotor has many operational disadvantages [1]. First, it operates exposed and close to the ground. This makes it dangerous to anyone and anything that gets in its way. Second according to U.S. Army safety reports, 20% of all peacetime helicopter accidents are caused by tail rotors [2]. Most of these crashes were caused by tail rotor strikes, tail rotor failure or loss of tail rotor effectiveness (LTE), which cause sudden and complete loss of directional control. Finally tail rotors are noise and being noise is not good for military, law enforcement forces or commercial users who must operate in populated areas.

Due to some of the disadvantages of the tail rotor, new anti-torque configurations were developed. One of the helicopter configuration without a tail rotor is the tip jet rotor, where the main rotor is not driven by the mast, but from nozzles on the tip of the rotor blade; which are either pressurized from a fuselage-mounted gas turbine or have their own turbojet, ramjet or rocket thrusters. Although this method is simple and eliminates torque, the prototypes were less fuel efficient than conventional helicopters and produced more noise. The McDonnell XV-1 is an example of this kind of helicopter designed in the 1950's. But its control capabilities were poor [2]. Another helicopter configuration developed without a tail rotor is the counter rotating main rotor configuration. In this configuration the main rotors are turning in opposite directions to counteract the effects of torque on the aircraft. Big helicopters like the

tandem-rotor Chinook and the twin-rotor Kaman K-50 are some examples of this configuration. Another class used for smaller sized helicopters is the so called No Tail Rotor (NOTAR). It produces anti-torque by using the Coanda Effect and controlling the circulation on the tail boom and directed jet of air at the aft end of the boom of the helicopter.

The use of directed air to provide anti-torque control had been trailed as early as 1945 in the British Cierva W.9 [4]. The W.9 was an experimental helicopter with a three-blade main rotor. Torque compensation was achieved by a jet of air discharged from the port side of the rear fuselage and supplied by a fan which also cooled the engine. The jet was controlled by two vanes. This model was not satisfactory enough.

The use of circulation control tail boom goes back to early 1960's. J.G. Lee [13] invented a helicopter anti-torque mechanism which utilizes a flow of air to create a circulation on the tail boom of the helicopter, in which presence of the main rotor downwash induces side force which opposes the torque reaction of the main rotor.

The idea of using both circulation control tail boom and direct jet thruster in order to obtaining anti-torque was appeared in a Lockheed project called "Advanced Anti-torque Concept" in 1971 [3]. This system of Lockheed developed by the engineer Joe Valazquez was similar to today's NOTAR concept. His invention has a main rotor driven axial compressor fan feeding a flow of air through a diffuser and an enlarged duct to variable geometry nozzle at the aft end of the boom generating an anti-torque and has two circulation slots mounted on the tail boom to supplement the anti-torque. Here, both fan and diffusers are controlled by pedal as today's NOTAR concept.

MDHC started the NOTAR project in 1976. By that time the company name was called Hughes Helicopters. The company used the experimental results of the cylindrical circulation control rotor blade development studies performed in England. Then circulation control tail boom was designed and tested on a blade tracking whirl stand [3]. The tail boom was internal-blowing and single-slotted. The slot width was less than a half inch and was located 140 degrees right side of the boom's top center [9].

The results of the tests showed that circulation control tail boom can be applied to helicopters. In the experiments, it was found that in order to obtain the optimum lift, the slot jet air velocity should be approximately 3.5 times more of the maximum downwash velocity and the slot

width should be between 0.15 to 0.8 inch. Also in these experiments it was found that the strength of the discharge through the slot can be described with a number called momentum coefficient and its value should be nearly 0.4 for an efficient tail boom [14].

While the whirl stand test results were good enough, flight tests were performed in 1978. Flight tests were done on a OH-6A helicopter keeping its tail rotor and installing a circulation control tail boom externally with air supplied by an electrically driven fan. It was shown that the boom interacted with the main rotor downwash in steady, controllable and a predictable manner. Addition of the boom decreased the tail rotor thrust nearly by 1/4 and the tail rotor power nearly 1/2. Vertical rate of climb performance increased but sideward or backward flight performance decreased [3].

In 1981, the entire OH-6A tail boom and tail-rotor were replaced by a fan, circulation control tail boom and direct jet thruster. In this application a Eurocopter fenestron fan [6] was used without optimization as it was about the right size and flight worthy. Fan pitch angle and thruster opening was controlled by the pilot pedal and they were coordinated so as to keep constant pressure inside the boom. But the flight test of the OH-6A-NOTAR demonstrator helicopter was not successful as it was expected. Although it was estimated that 60% of the total anti-torque requirement would be produced by the boom, only 20% of the anti-torque was obtained from the boom. In order to solve the lift inefficiency problem, analytic and experimental methods were used [15]. For analytic solution, two dimensional strip analysis was performed in modeling the elements of the circulation control to represent the aircraft and the rotor flow field. The VSAERO program, which uses low order panel method, was used in this study. As a result, it was observed that more circular cross section was needed. In addition, many whirl stand hover out ground effect tests were accomplished. It was seen that the actual flow is much more complicated than it was predicted. The main reason of the inefficiency was the effect of the airflow coming from the forward fuselage [15]. Therefore, two fences at both end of the slots were installed as a flow insulator. By this method good lift efficiencies were achieved. But on the other side, in forward flight they caused abrupt increase in drag and decrease in yaw stability [16].

In order to get rid of the fences, a scaled model flight visualization experiment test was done in a 1000 gallon water tank facility of MDHC in 1985. At the end of several configurations and tests, it was observed that the attached flow without fences can be obtain by adding second

slot of equal length on the 70 degree from the booms top center. The second slot energize the flow to keep attached beyond the 90 degree separation point, where the second slot become effective. Since no additional air flow was required, total slot exit area was kept constant [16].

After two slotted approach the NOTAR concept gave good performance and the company focused on the structural design. Firstly, individual components of the NOTAR system were designed, tested and evaluated. Then the whole system performance was tested and evaluated. Each components of NOTAR was tested, evaluated and optimized. Fan inlets were optimized for minimum total pressure loss, minimum drag, and non uniformity. Very low pressure differential across the inlet with a ninety degree deflection of the air flow has been obtained. Second, variable pitch, axial flow fan, which provides pressurized air for tail boom was developed. On the OH-6 NOTAR demonstrator, the fenestron fan had been used, and it was not optimized for this application. The fan should be operate wide range of flow conditions, but the efficiency of that fan was only about 45% on those conditions. Therefore a new fan, which can operate over a wide range of flow conditions was developed. The new fan had an efficiency of about 85%. Achieving good efficiencies on different flow conditions was an important factor for the NOTAR development. In fact, the MD 530N was certified after the design of the new fan. On the other hand many wind tunnel tests were accomplished in order to understand the air flow on the circulation lift tail boom and to improve the performance of the boom. Therefore, lift and drag coefficients were found and recorded for different momentum coefficients, angle of attack and boom aspect ratio (slot length/boom diameter) [15]. Also different non-circular booms were developed some of which was more efficient than circular cross section tail boom [9].

During the 5 years period, system performance tests were conducted. The tests were done on the ground either with an internal flow test rig or wind tunnel models and on flight with instrumented helicopters. On the ground rig tests, maximum thruster forces of 1400 lbs were achieved which was required for 1a 80 degree pedal turn on 45 knot wind condition in any direction. During the tests, the off-design conditions of circulation control tail boom were analyzed and optimized, especially low speed flight in ground effect condition was analyzed, which is hard to model analytically. Many flight tests were performed with instrumented OH-6 and MD 530N helicopters. Boom pressure data were recorded for hover trim, low speed sideward flight in ground effect and out of ground effect and level forward flight conditions. In these tests, the sectional and total circulation control tail boom aerodynamic loads were

determined. For example; since main rotor downwash is slower in ground effect, boom side force and thus yawing moment is reduced when it is compared to out of ground effect. Also the right sideward flight effect on tail boom yaw moment production was determined during the flight tests. It was observed that the boom anti-torque production decreases with right sideward flight. At approximately 20 knots right flight condition, the boom could not produce anti-torque anymore. Also the boom anti-torque production on level forward flight was also determined in these tests. It was observed that at a speed of 60 knots, the tail boom produces 20% of the yaw moment it was produced in hover. And it increases to 30% of its hover value by the speed of 110 knots [6]. Also at the end of so many flight tests, strake was installed on the left side of the boom which improved the tail boom performance especially on right sideward flight. Addition of the strike contributes 10% reduction of the fan power [7].

In addition to these, some flight tests were performed in order to compare hovering performance of first generation production NOTAR system-equipped helicopter MD 530N to a conventional tail rotor helicopter MD 530F. Both helicopters have identical main rotor, forward fuselage and engine configuration. The only difference between the two helicopters is the anti-torque system. Results of the flight tests showed that two helicopters require the same power during hover in ground effect and out of ground effect. The main rotor of the MD 530N is more efficient because of less main rotor flow interaction, therefore it requires less power. But NOTAR fan needs more power when it is compared to conventional tail rotor [7].

For stabilization, more than 50 tail configurations were tried. But two problems could not be solved by those configurations until an augmentation system was developed. The problems were static instability in yaw axis during 60 knots descents and dynamic dutch roll instability during level flight over 90 knots and climbs above 80 knots. In order to solve these problems, a stability augmentation system (Yaw SAS), which controls the right vertical stabilizer, was developed for yaw axis [3].

Also acoustic flight tests were accomplished in 1992. The results showed that NOTAR helicopters are 50% quieter than any comparable helicopter. The reason is that the NOTAR fan is inside the fuselage and its tip speed is lower than tail rotors [6]. Also there is no main rotor-tail rotor flow interaction on a NOTAR helicopter.

Today there are three certified NOTAR helicopter type and all of them are designed by MDHC. They are called MD 530N, MD 600N and MD 900.

2.2 NOTAR System Description

The NOTAR is an anti-torque system which is made up of an enclosed fan that is driven by the main transmission, a circulation control tail-boom, direct-jet thruster and horizontal stabilizer with two vertical stabilizers (H- Tail) as it is seen on figure 2.1. In this system, low pressure air is produced in through an air intake located at the top of the airframe to the rear of the main rotor shaft by a variable pitch fan located in the aft section of the fuselage. This low pressure air is blown axially along the tail boom, providing air for both circulation control and the direct jet. A part of the air is ejected from thin horizontal slots at the right side of the boom. This air flow follows the contour of the tail boom and induces the main rotor wake do the same figure 2.2. This effect is called Coanda Effect and makes the boom behaves like an airfoil which creates lift in the direction needed for anti-torque. The remaining air is ejected from the direct jet thruster at the aft section of the tail boom and this supports the required anti-torque and provides maneuverability for yaw control and directional change [8]. In forward flight, the majority of the anti-torque is provided by the vertical stabilizers [17]. The variable flow fan pitch angles, direct jet thruster and the vertical stabilizers are all controlled by pilot pedals.

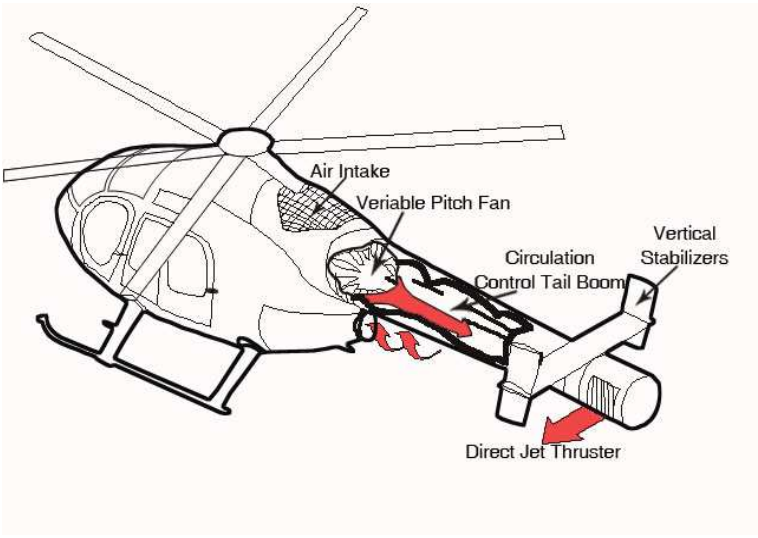

Figure 2.1: A General Schema of NOTAR Helicopter

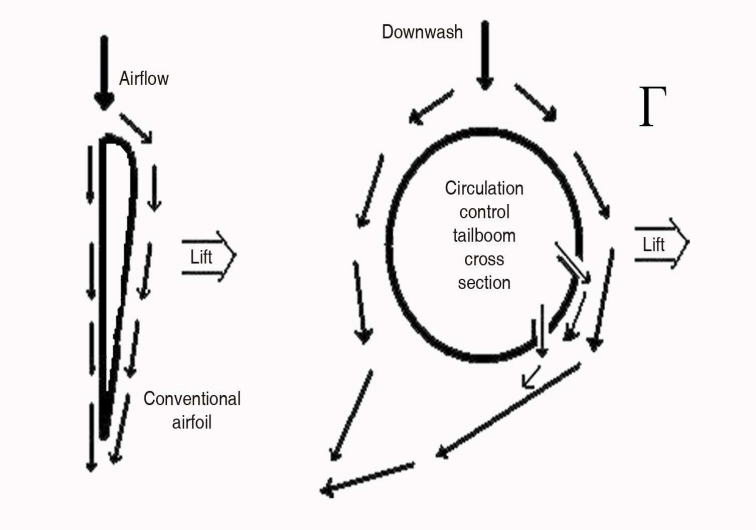

Figure 2.2: Circulation Lift

2.3 Components of the NOTAR

The NOTAR anti-torque system is composed of an air inlet, fan, diffuser, circulation control tail boom, direct jet thruster, horizontal and vertical stabilizers as it is seen on figure 2.1.

2.3.1 Fan Air Inlet

Fan air inlet is a single opening aft and below of the main rotor hub. This inlet provides air flow for NOTAR fan with a minimum total pressure losses and non uniformity [6]. Downwash air flow is deflected approximately 90 degree in order to be on the same axis with the fan axis. Minimal total pressure loss is provided with an optimum design in a wide range of flight conditions according to so many wind tunnel tests.

2.3.2 Fan and Diffuser

Fans, that are used for NOTAR anti-torque systems are low pressure, variable pitch, axial flow compressor fans that produces air flow for circulation control tail-boom slots and direct jet thruster. The fan is located on the aft section of the fuselage and driven from the main transmission. The fan operates over a wide range of flow conditions to provide the required

pressure and required mass flow rate which varies depending on the flight regime. For example in left pedal turn or right sideward flight the boom needs more mass flow and the fan pitch must be very high because of high anti-torque requirement. In hover condition, fan pitch must be in mid level so as to provide enough pressure and to control mass flow enough for tail boom slots and thruster. But in high speed forward flight, since most of the anti-torque is provided by the vertical stabilizers, the fan blades must be very low pitch [6]. The fan is designed to provide nearly constant pressure inside the boom as the flow through thruster nozzle area varies. It is known that maintaining 0.5 psi above the outside atmospheric pressure is sufficient [8]. In fact, fans used in today's NOTAR systems are capable of maintaining a boom pressure of one psi above the outside air pressure [3]. When high anti-torque is required fan increases the air flow rate keeping internal boom pressure constant as much as possible [6]. On the other side since the fan is installed internally, it is not effected from outside inflow variations.

The fan's rotor energizes the airflow in a rotational flow. And the fixed geometry stator vanes convert the rotor swirl energy into axial flow energy. The stator and diffuser assembly is located at the front of the boom and streamline the airflow exiting from the fan, increase fan performance and quiet the fan noise.

2.3.3 Circulation Control Tail Boom

Circulation control tail boom is a part of NOTAR system which produce anti-torque based on the Coanda effect. The tail boom is under the main rotor wake and it has two slots where low pressure of air produced by the fan exits. The low pressure air gets out from two tail boom slots, causing the rotor wake to adhere to the counter of the boom. This produces force which can also describe via circulation lift. This force provides majority of the anti-torque force required to hover.

The air flow can stay attached to tail boom if the jet velocity blowing from the slots is four times the average downwash velocity. The internal boom pressure of only half psi above the outside air pressure is sufficient for this [3].

This system is self-compensating; when the rotor system is producing higher torque it is also producing higher downwash with resultant lift (anti-torque). At low torque, less downwash is

Figure 2.3: Circulation Control Tail Boom

present and the tail boom produces less lift at a time when less anti-torque is required [18].

In hover, the circulation control tail boom (figure 2.3) provides approximately 60% of the anti-torque force required [8]. Creating lift via circulation control tail boom is more efficient when it's compared with creating lift by Jet thruster. So its good to have more effective circulation control tail boom.

2.3.4 Direct Jet Thruster

The direct jet thruster (2.4), which is located at the aft end of the circulation control tail boom, receives the pressurized air flow from the boom, directs it to either side of the end of the tail boom and discharges it perpendicular to the boom axis in various amounts with variable exit valve so as to provide required amount of side force [6]. By this side force, it provides directional control for maneuvering and supplements the required anti-torque in addition to that circulation control tail boom provides. The direct jet thruster is composed of two cones (figure 2.5). The non rotating inner thruster cone has two large openings on either side and consists of a cascade system of airfoils which turns the airflow entering with the axial direction parallel to boom and exiting either left or right openings and perpendicular to the boom axis in an efficient way. The rotating cone has a single opening and as it rotates a controlled amount of airflow exits from the stationary cone and thus varies the thruster output

and direction of thrust. The rotating cone is controlled by pilot's pedal.

Figure 2.4: Direct Jet Thruster, Vertical and Horizontal Stabilizers

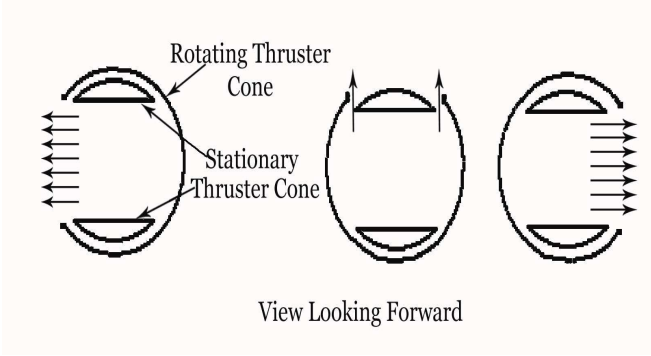

Figure 2.5: Direct Jet Thruster Inside

2.3.5 Horizontal and Vertical Stabilizers

The vertical stabilizers are connected to the pilot's pedals (figure 2.4). The left stabilizers moves through approximately 30 degree of motion and provides sufficient control force for autorotation [17]. Most of NOTAR versions right vertical stabilizer is optionally controlled by Yaw Stability Augmentation System (YSAS). It is enhance handling qualities. Although in hover their effect is low, in forward flight most of the required anti-torque and yaw control is provided by vertical stabilizers.

The horizontal stabilizer is set at a fixed angle of incidence and attaches atop the tail boom just forward of the thruster. At each end of the horizontal stabilizer there is a vertical stabilizer.

CHAPTER 3

NOTAR MODEL DEVELOPMENT

The mathematical model of the NOTAR anti-torque system is developed for real-time simulation. Such a model has not been reported in open literature.

It is a well known fact reported by pilots that the NOTAR system and the traditional tail Rotor flight characteristics have many differences. In traditional tail rotor concepts the tail rotor is the main anti-torque and the yaw maneuver control source during most of the flight conditions. Other parts are only supplementary. On the other hand the NOTAR system is composed of three major anti-torque devices; circulation control tail boom, direct jet thruster and vertical tails and proportion of the anti-torque produced by these elements depends on the mode of the flight.

In hover, the circulation control tail boom provides the majority (approximately 60%) of the required main rotor anti-torque. [3], [2], [6], [7], [8], [9], [10], and the direct jet thruster produces the remaining. In transitional forward flight, the main rotor downwash flows above the tail boom and only a small amount of the force is created by the tail boom. Thus the major anti-torque device is the direct jet thruster in that condition. In high speed forward flight, vertical stabilizers provide the majority of the anti-torque, however directional control remains as a function of the direct jet thruster [17]. Therefore, especially during flight mode changes, more pedal control is needed for a NOTAR helicopter. In addition, the boom anti-torque generation varies depending on the free stream wind condition. Therefore the supplement work on the thruster may change much especially during take off and landing and this causes also unpredicted big pedal control need. On the other side, in traditional tail rotor concepts the flight modes and air conditions causes only change in efficiency or amount of thrust production of the tail rotor. But it continues to be the major anti-torque device. Also the thrust

changes of the tail rotor during the flight mode changes are generally predictable. Therefore NOTAR has different characteristics and the mathematical model should be different from the tail rotor models.

The development of the mathematical model of a NOTAR depends on complicated aerodynamic solutions. In order to solve the problem firstly the flow of air inside the tail boom is analyzed by dividing into 6 control volumes and specifying 8 section. The air enters the boom from the air inlet, it is pressured by the fan, stators and diffuser, and exits as a jet flow from the slots and direct jet thruster. Then, the airflow outside the tail boom is analyzed. Therefore, thrust produced by direct jet truster and circulation control tail boom is solved. Finally, vertical tail effect is added to the model.

When each part of the NOTAR system is considered separately the following problems needs to be solved: First, the flow rate of the air passing through the boom needs to be calculated. Then the pressure ratio of compressor fan inside the boom is needed to be solved. The mass flow rate, velocity and the energy of the air ejecting from the slots is to be calculated. Also total pressure of air the flows out from direct jet thruster is a question waits for answer. On the other hand, the downwash of the main rotor must be solved. In addition to these, the whole system needs to be analyzed and the interactions are to be calculated. The created lift when air is ejected form the slots inducing the downwash of the main rotor by Coanda effect is to be calculated. The boom anti-torque production which changes with different flight modes and different atmospheric conditions is another problem. The boom internal pressure and air flow rate differentiation depending on the pilot pedal inputs must be clarified. In addition the contributions due to vertical stabilizers should also be calculated.

Although the problem is complicated, the model needs to be simple enough to be run in real-time simulation, yet represent the actual dynamics.

3.1 The Air Flow Inside the Tail Boom

The model development is started with a goal to solve the air flow which enters from the NOTAR inlet, is pressurized by the fan, and goes out as a jet flow from the slots and direct jet thruster. Therefore, the system is divided into some control volumes. Totally 6 control volumes defined by 8 sections are found to be enough in order to solve this flow with feasible

assumptions.

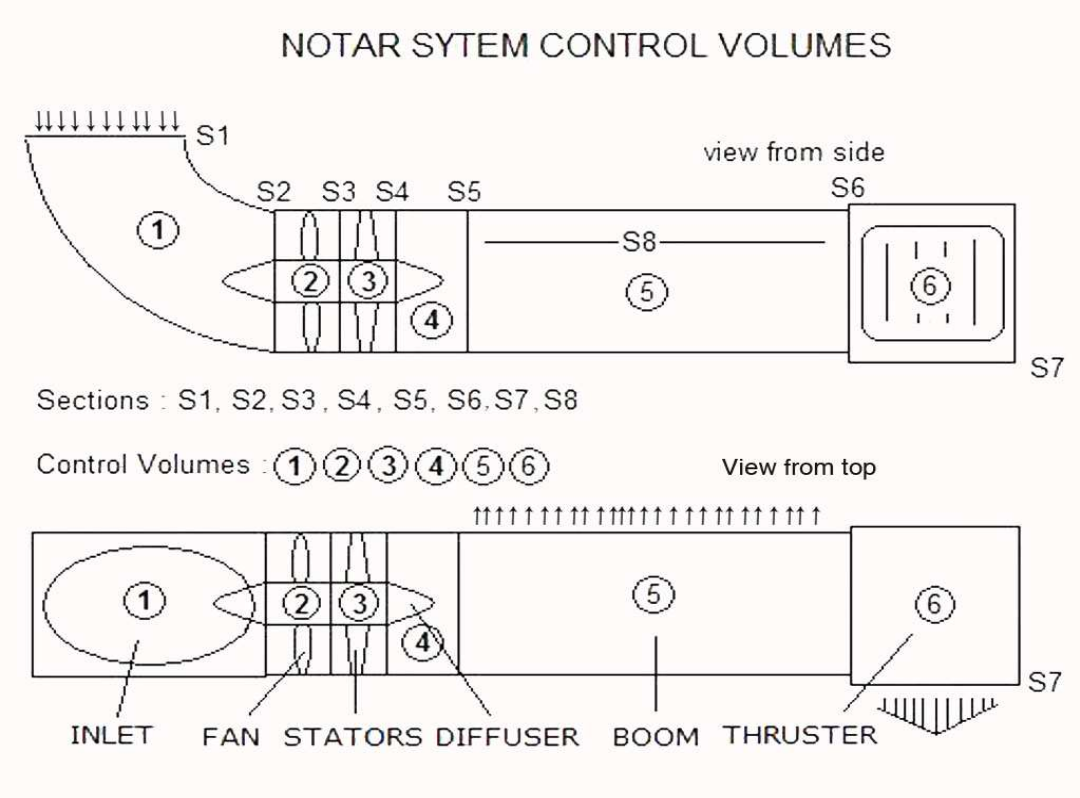

Figure 3.1: A general schema of NOTAR control volumes

CONTROL VOLUME 1 : NOTAR AIR INLET : Downwash of the main rotor enters from the section 1, deflects approximately 90 degree and prepare air for NOTAR fan.

CONTROL VOLUME 2 : NOTAR FAN : The air enters from section 2 and the total pressure of it is increased (angular momentum is increased) by the fan and exits form section 3.

CONTROL VOLUME 3 : STATORS : The air which has axial and swirl velocity produced by the fan enters from section 3 and it is turned into axial flow of air (angular velocity is turned into pressure) and exits from section 4.

CONTROL VOLUME 4 : DIFFUSER : The air enters from the section 4 and it is pressurized (some of the momentum energy is turned into pressure) and exits from section 5.

CONTROL VOLUME 5 : INSIDE OF THE TAIL BOOM : The air flow enters from section 5 and some of it exits from slots on the right side of the boom (section 8) and the remaining

air exits from section 6.

CONTROL VOLUME 6 : THRUSTER : Pressurized air coming from the boom in section 6 exits from the opening in section 7, producing thrust for the required anti-torque.

3.1.1 Control Volume 1 : NOTAR Air Inlet

First control volume is the one between sections 1 and 2. It is the NOTAR Air Inlet where the downwash of the main rotor enters the boom and turns approximately 90 degree so that it is on the same axis with the fan. The amount of the total pressure of the air flow varies depending on flight modes.

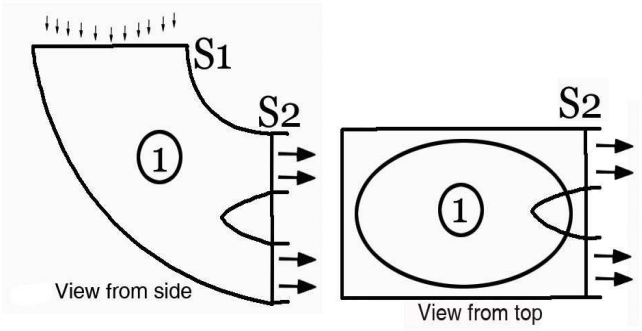

Figure 3.2: CV1 NOTAR Air Inlet

Pressure at section one, P_1, can be found by the Bernoulli Equation if velocity V_1 is known.

$$P_1 = P_0 - 1/2\rho_1 V_1^2 \tag{3.1}$$

where P_0 is the outside air pressure.

Since all of the airflow which enters from section 1, exits from section 2, conservation of mass can be applied inside the control volume. Experiment results show that velocities through the boom are no more than 0.3 Mach [9]. Therefore the flow can be assumed incompressible throughout the model which means density ρ is constant. Thus;

$$V_2 = V_1 A_1 / A_2 \tag{3.2}$$

If incompressible, inviscid flow assumption is used then the Bernoulli Equation can be applied;

$$P_1 + 1/2\rho V_1^2 = P_2 + 1/2\rho V_2^2 \tag{3.3}$$

In fact, in 90 degree turn ducts, total pressure can not be conserved because the skin friction and losses due to eddying or separated flow are rather high. Therefore 3.3 becomes;

$$P_{T2} = P_{T1} - \Delta P_{TI} \tag{3.4}$$

where;

$$\Delta P_{TI} = K_I(1/2\rho V_2^2) \tag{3.5}$$

Thus total pressure is;

$$P_{T2} = P_1 + 1/2\rho V_1^2 - 1/2\rho V_2^2 K_I = P_2 + 1/2\rho V_2^2 \tag{3.6}$$

and pressure in section 2 is;

$$P_2 = P_1 + 1/2\rho(V_1^2 - V_2^2 - V_2^2 K_I) \tag{3.7}$$

where P_{T1}, P_{T2} are total pressures in sections 1 and 2, K_I is a non dimensional loss coefficient and ΔP_{TI} total pressure loss on the inlet.

3.1.2 Control Volume 2 and 3 : NOTAR Fan and Stators

The second control volume is the one between sections 2 and 3. In this control volume the axial flow fan pressurizes the airflow which comes from the inlet. In fact, it is known that the fan aims to keep constant pressure inside the boom (Between 0.5 to 1 psi above the outside air pressure) [3],[8]. The fan has variable pitch blades controlled by pilot pedals so that to change the mass flow rate depending on the anti-torque requirements and to keep a constant pressure inside the boom when the thruster opening varies with pedal inputs [8].

First the axial flow fan is analyzed. It is known that axial flow fans are analyzed by using either ”free vortex flow theory” or ”arbitrary vortex flow theory” [20].

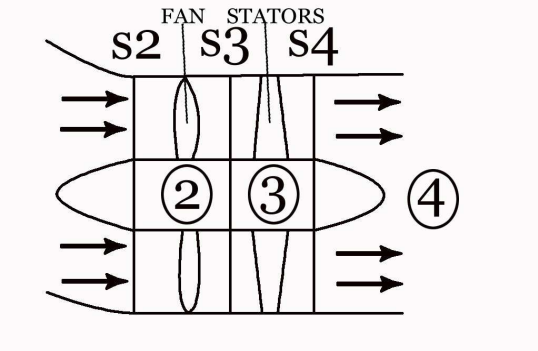

Figure 3.3: CV2-CV3 NOTAR Fan and Stators

Arbitrary vortex flow theory is mostly used in high pressure rise rotor designs [20]. On the other hand free vortex flow is assumed when designing ducted axial flow fans. Since the NOTAR fan is low pressure and ducted, free vortex flow assumption can be used in calculations.

In Free vortex flow, it's assumed that the airflow velocity has no radial component. The absolute tangential velocities in front and behind the fan vary inversely with the radius, i.e,

$$V_\theta = Cnst/r \tag{3.8}$$

A free vortex rotor is also characterized by a uniform total energy rise across the annulus. This flow is achieved when both the total pressure rise and axial velocity component remain constant along the blade span.

Provided the design meets free vortex flow conditions, the midspan station is a possible choice for calculations [20]. Because theoretical total pressure rise and axial flow component are constant with radius. Therefore mid span station is used on fan calculations.

On the axial flow fan, the flow of air is parallel to the axis of the rotor. Air approaches the rotor in the axial direction and leaves it with a rotational velocity component due to the work done by the rotor.

After the axial flow fan, there are stators which turns swirl velocity component of the air produced by the fan into axial flow by pressurizing the air. They are shown in control volume 3.

In mid span station the total pressure of each section is given as;

$$P_{T2} = P_2 + \frac{1}{2}\rho V_a^2 \tag{3.9}$$

$$P_{T3} = P_3 + \frac{1}{2}\rho V_a^2 + \frac{1}{2}V_{\theta_s}^2 \tag{3.10}$$

$$P_{T4} = P_4 + \frac{1}{2}\rho V_a^2 \tag{3.11}$$

where P_{T2}, P_{T3}, P_{T4} are total pressures on sections 2, 3 and 4, P_2, P_3, P_4 are static pressures on sections 2, 3 and 4, V_a is the axial velocity which is equal to V_2, V_3, V_4 (velocities on sections 2, 3 and 4) from continuity and V_{θ_s} swirl velocity component.

The overall change in total pressure can be written as,

$$P_{T4} - P_{T2} = \Delta P_{Tth} - \Delta P_{Tf} - \Delta P_{Ts} \tag{3.12}$$

where ΔP_{Tth} is theoretical total pressure rise, ΔP_{Tf} is the fan loss and ΔP_{Ts} is the stator loss.

Dividing equation 3.12 by $\frac{1}{2}\rho V_a^2$;

$$\frac{P_{T4} - P_{T2}}{\frac{1}{2}\rho V_a^2} = K_{th} - K_f - K_s \tag{3.13}$$

From equation 3.13 total pressure rise across the fan is;

$$P_{T3} - P_{T2} = \frac{1}{2}\rho V_a^2 K_{th} - K_f \tag{3.14}$$

From equation 3.9 and equation 3.10 total pressure rise across the fan;

$$P_{T3} - P_{T2} = P_3 - P_2 + \frac{1}{2}\rho V_{\theta_s}^2 \tag{3.15}$$

Therefore;

$$\Delta P = P_3 - P_2 = \frac{1}{2}\rho V_a^2 (K_{th} - K_f - \epsilon_s^2) \tag{3.16}$$

where ϵ_s is swirl coefficient on the downstream of the fan and;

$$\epsilon_s = V_{\theta_s}/V_a \tag{3.17}$$

Thus pressure downstream of the fan P_3 becomes;

$$P_3 = P_2 + \frac{1}{2}\rho V_a^2 (K_{th} - K_f - \epsilon_s^2) \tag{3.18}$$

Work done by the fan is;

$$W = (P_{T3} - P_{T2}) 2\pi V_a r dr \tag{3.19}$$

Work done as input by the fan is ΩdT and it is;

$$\Omega dT = \rho V_a 2\pi r dr(V_{\theta_s})\Omega r \tag{3.20}$$

Equating the equations 3.19 and 3.20;

$$(P_{T3} - P_{T2} + \Delta K_f) = 2\pi r dr V_a = \rho V_a 2\pi r dr V_{\theta_s}\Omega r \tag{3.21}$$

$$\Delta P_{Tth} = \rho\Omega r(V_{\theta_s}) \tag{3.22}$$

Non dimensionally;

$$K_{th} = \frac{2}{\lambda}(\epsilon_s) \tag{3.23}$$

where;

$$\lambda = V_a/\Omega r \tag{3.24}$$

The momentum analysis of the fan is already shown. Here the blade element analysis of the fan is given. The velocity the blade receive is the resultant velocity (V_m) and it is shown in 3.4.

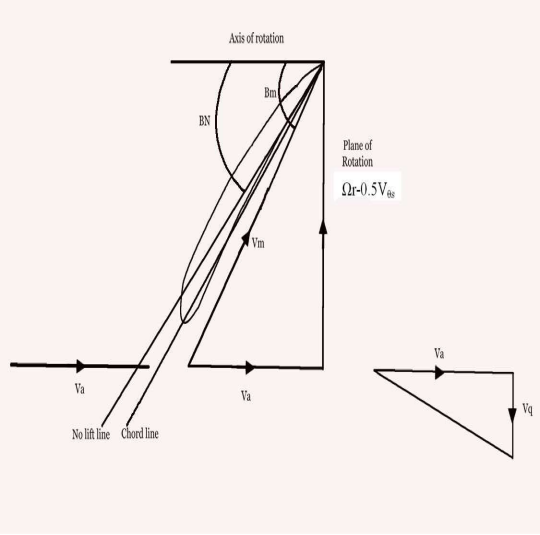

Figure 3.4: Fan Blade Element

From the figure it can be seen that;

$$tan\beta_m = \frac{\Omega r - \frac{1}{2}V_{\theta_s}}{V_a} \tag{3.25}$$

In another way;

$$tan\beta_m = \frac{1 - \frac{1}{2}\epsilon_s\lambda}{\lambda} \tag{3.26}$$

where β_m is angle that relative velocity V_m makes with fan blades.

From the blade element solution according to reference [20] using the figure 3.4

$$c_L\sigma = 2\epsilon_s cos\beta_m \tag{3.27}$$

Lift coefficient can be expressed as;

$$c_L = msin(\beta_m - \beta_N) \tag{3.28}$$

where angle of attack (α) is;

$$\alpha = \beta_m - \beta_N \tag{3.29}$$

where β_N is the value of β_m for no lift condition of the fan. In another words it is the angle between axis of rotation and an imaginary line which the blade can not produce lift. Therefore it is geometrical value depends on the pedal input. $\beta_m - \beta_N$ is the incidence relative to no lift line. Since the fan has a low cambered airfoil blade lift curve slope (m) can be taken as 5.7.

According to reference [20] blade element solution together with the momentum consideration, swirl coefficient ϵ_s can be found depending on flow coefficient λ ;

$$\epsilon_S = \frac{2sin\beta_N(\frac{cot\beta_N}{\lambda} - 1)}{\frac{4}{m\sigma} + cos\beta_N} \tag{3.30}$$

And;

$$V_{\theta_s} = \epsilon_s V_a \tag{3.31}$$

Since β_N is a value depends on pedal input, fan properties can be found depending on the axial flow rate and pedal input.

As a next step NOTAR fan and stator losses are analyzed.

According to reference [20] the mean total pressure loss coefficient K_f has a relation as;

$$\frac{K_f}{K_{th}} = (\frac{C_{D_P}}{C_L} + \frac{C_{D_S}}{C_L})(\frac{\lambda}{COS^2\beta_m})_{MS} \tag{3.32}$$

where C_{D_P} is the profile drag coefficient at mid blade span C_{D_S} is the secondary drag coefficient and it can be calculated as;

$$C_{D_S} = bC_L^2 \tag{3.33}$$

where b is taken between 0.018 to 0.015. For high Reynolds numbers (as this case) 0.015 is a better choice. Also C_{D_P} can be predicted from figure B1 on Appendix B since low cambered flat under surface airfoil is used in NOTAR fan. Therefore it can be predicted according to lift coefficient. For example if lift coefficient is close to 0.8, then C_{D_P} can be taken as 0.01.

Stator losses can be found from the figure B2 on Appendix B. Total pressure losses of the stators depend on flow coefficient at the mid blade span λ, swirl coefficient ϵ_s again at the mid blade span and theoretical total pressure rise coefficient of the fan K_{th}.

$$K_s = aK_{th}\lambda \tag{3.34}$$

Therefore;

$$P_4 = P_3 + 1/2\rho(V_{\theta_s}^2 - V_a^2 K_s) \tag{3.35}$$

3.1.3 Control Volume 4 : Diffuser

There is a diffuser assembly as a fairing of the fan on downstream of the stators. It has two functions: One is increasing the static pressure of the airflow inside the boom. Other is decreasing the velocity of the flow in a steady manner. In other words airflow coming from stators enter from section 4, and they are pressurized and their velocity is decreased and then they exit from section 5. There is also some loss inside the diffuser and it is defined as non dimensional loss coefficient K_d.

From continuity;

$$V_5 = V_a A_4 / A_5 \tag{3.36}$$

Here incompressible, inviscid flow assumption is used and Bernoulli Equation can be used including the losses;

$$P_5 = P_4 + 1/2\rho V_a^2 - 1/2\rho V_a^2 K_d - 1/2\rho V_5^2 \tag{3.37}$$

3.1.4 Control Volume 5 : Tail Boom

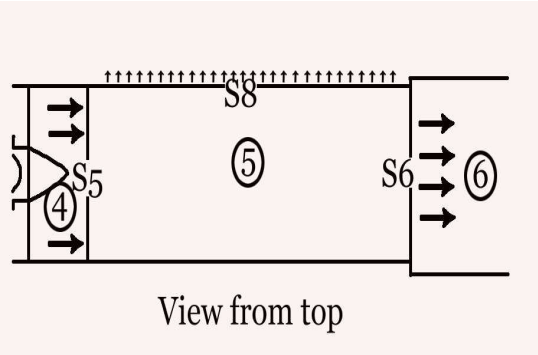

Figure 3.5: Tail Boom

Fifth control volume is bounded by section 5 in front, section 8 on the right side and section 6 on the aft. Section 5 is the place where enters the air which pressurized after the fan, stators and diffuser. In section 8, there are two slots where the air exiting as jet flow which induces the main rotor downwash providing side force because of Coanda effect. Properties of section 8 is analyzed on chapter 3.2. Section 6 provides air flow for direct jet thruster. The aerodynamic solution on this control volume can be found as follows.

From the conservation of mass;

$$V_6 = (V_5 A_5 - V_8 A_8)/A_6 \tag{3.38}$$

Since the slot velocities are not higher than 0.3 Mach the flow can be assumed incompressible. Then from conservation of momentum equation;

$$V_5^2 A_5 = V_6^2 A_6 + V_8^2 A_8 + V_5^2 A_5 K_b \tag{3.39}$$

where K_b is non dimensional loss coefficient of the boom.

K_b can be found using Darcy Weisbach equation which relates the pressure loss due to friction along a given length of pipe to the average velocity of the fluid flow.

$$\Delta P = \frac{\rho V^2}{2} \frac{fl}{d} \tag{3.40}$$

where l is the length of the boom d is the diameter of the boom f is the friction factor from

the Moody chart and it depends on material properties, the Reynolds number and the regime of the flow.

From equationn 3.40 it can be seen that

$$K_b = \frac{fl}{d} \tag{3.41}$$

Thus;

$$P_6 = P_5 + 1/2\rho V_5^2 - 1/2\rho V_5^2(K_b + K_m) - 1/2\rho V_5^2 \tag{3.42}$$

where K_m is loss of total pressure due to slot exits.

3.1.5 Control Volume 6 : Direct Jet Thruster

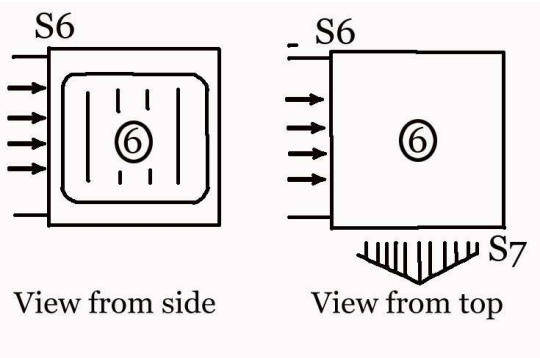

Figure 3.6: CV6 Direct Jet Thruster

The final control volume is bounded by section 6 and section 7 where the air flow comes from tail boom and turns 90 degrees to the left or right and exits outside from the thruster openings. Area 7 varies with pilot pedal controls. Since there are cascades of airfoils to turn the flow; it can be assumed that the total pressure drop inside the control volume is small.

From conservation of mass assuming incompressible, inviscid flow, we can use quasi one dimensional continuity equation from [21];

$$V_7 = V_6 A_6 / A_7 \tag{3.43}$$

where; V_7 velocity of jet air ejecting from thruster, A_7 area of thruster opening which varies with pilot pedal input.

Thruster exit velocity V_7 also has a relation with inlet airflow velocity V_1, and slot jet air exit velocity V_8 from the law of conservation of mass. The amount of the air enters to the boom equals to the amount of the air exits. Therefore;

$$V_1 = (V_7 A_7 + V_8 A_8)/A_1 \tag{3.44}$$

Also Bernoulli Equation can be applied in this control volume because incompressible, inviscid, steady flow assumptions can be used. Therefore;

$$P_7 + (1/2)\rho V_7^2 = P_6 + (1/2)\rho_6 V_6^2 - (1/2)\rho_6 V_6^2 K_t \tag{3.45}$$

Where P_6 is internal boom pressure, P_7 is pressure of the air ejecting from the thruster and K_t is non dimensional loss coefficient of the thruster.

Then the pressure of the air jet blows out from section 6 (thruster) becomes;

$$P_7 = P_6 + (1/2)\rho V_6^2((1 - A_6^2/A_7^2) - K_t) \tag{3.46}$$

Thrust is produced on direct jet thruster by ejecting pressurized air to either sides from the opening of the thruster. The side force appeared can be derived by conservation of momentum and energy equations as it is described in [22]. Using the control volume 6, the thrust formula becomes;

$$F_{thruster} = \dot{m}_7 V_7 - \dot{m_0} V_0 + (P_7 - P_0)A_7 \tag{3.47}$$

since $\dot{m}_0$ equals to zero;

$$F_{thruster} = [\rho V_7^2 + (P_7 - P_0)]A_7 \tag{3.48}$$

3.2 Air Flow Outside The Circulation Control Tail Boom

Circulation control is a method to create lift on a body by controlling the position of downstream boundary layer separation point of the body and this controls the circulation and controls the lift on the body. In conventional airfoil the sharp trailing edge is the rear stagnation point (Kutta condition). Circulation thus lift is controlled by the angle of attack of the airfoil. But the separation point on the circulation control airfoil can be controlled via blowing a thin jet of air tangential over its rounded trailing edge [9]. Because of the Coanda Effect, which is the tendency of a fluid jet to adhere to a solid wall even when the wall curves away from the jet's axis, a thin layer of laminar jet flow produced from the longitudinal slots, exits adjacent to the surface controlling the rear stagnation point pushing it toward the lower surface and thus creating the lift. This circulation control concept was directly applied to the NOTAR anti-torque system whereby the tail boom of the helicopter pressurized in order to obtain jet air flow and became a low-aspect ratio wing operating in a flow field generated by the main rotor.

The circulation control tail boom can be characterized like lifting flow over a cylinder by which lift and drag can be found. The aerodynamic solution of lifting flow over a cylinder can be found as follows:

Lifting flow over a cylinder can be synthesized by addition of the non lifting flow over a cylinder and a vortex flow of a strength Γ [21].

A non lifting flow over a cylinder is a combination of a uniform flow and by a doublet flow [21].

The stream function for an incompressible uniform flow in terms of polar coordinates is

$$\psi = V_\infty r sin\theta \tag{3.49}$$

The stream function of a doublet flow which is a special case of a source-sink pair can be described as;

$$\psi = -\frac{\kappa}{2\pi}\frac{sin\theta}{r} \tag{3.50}$$

The combination of uniform flow with velocity V_∞ and doublet flow strength of κ;

$$\psi = V_\infty r sin\theta - \frac{\kappa}{2\pi}\frac{sin\theta}{r} \tag{3.51}$$

Let,

$$R^2 = \frac{\kappa}{2\pi V_\infty} \tag{3.52}$$

Then,

$$\psi = V_\infty r sin\theta (1 - \frac{R^2}{r^2}) \tag{3.53}$$

Therefore the velocity distribution on the surface of the cylinder is;

$$V_\theta = -2V_\infty sin\theta \tag{3.54}$$

On the other hand, in vortex flow all streamlines are concentric circles to a point and the velocity on any streamline is constant whereby it changes one streamline to other inversely with distance from the center. Thus;

$$V_\theta = \frac{constant}{r} \tag{3.55}$$

Where the strength Γ of the circulation can be found by the negative line integral of velocity around a closed curve in the flow. The sign convention is that the vortex of positive strength rotates in the clockwise direction.

Line integral of a spinning cylinder is ;

$$\Gamma = -\oint V * ds = V_\theta (2\pi r) \tag{3.56}$$

Thus the stream function of flow over a spinning cylinder is;

$$\psi = \frac{\Gamma}{2\pi} lnr \tag{3.57}$$

In NOTAR tail boom there is a jet flow only approximately 90 degree of the boom surface. This causes boundary layer friction only $\frac{1}{4}$ of the cylinder surface, as if only quarter of the cylinder is spinning.

Therefore line integral on this condition is

$$\Gamma = V_\theta \frac{\pi}{2} r \tag{3.58}$$

The NOTAR tail boom can also be thought of a small cylinder spinning inside of a stationary cylinder. Here, only the right bottom side of the spinning cylinder is opened to the down wash air flow. The solution of this condition is also the same.

In addition to this, although equation 3.56 is derived for circular cylinders, it applies in general to cylindrical bodies of arbitrary cross section [21]. It can also be applied to airfoils. The important thing is the velocity field around that shape. Therefore looking the velocity field around circulation control tail boom, and the line integral of around the boom gives the same solution.

Now combining vortex flow over the tail boom and non lifting flow over it, the stream function becomes;

$$\psi = (V_\infty r sin\theta)(1 - \frac{R^2}{r^2}) + \frac{2\Gamma}{\pi} ln\frac{r}{R} \tag{3.59}$$

Velocity on the surface of the cylinder become;

$$V_\theta = -2V_\infty sin\theta - \frac{2\Gamma}{\pi R} \tag{3.60}$$

In fact when circulation strength over a circular cylinder is known, force produced per span can be found by using Kutta-Joukowski theorem given below;

$$F' = \rho_\infty V_\infty \Gamma \tag{3.61}$$

Therefore if the downwash velocity and the slot exit velocity is known, then the force produced by the circulation control tail boom can be calculated.

So as a next step exit velocity V_8 of the slot jet air is found.

The exit velocity of the slot jet air depends on the downwash velocity of the main rotor, tail boom inside pressure, boom momentum, boom diameter and slot width. Assuming incompressible flow, it can be said that density does not effect the velocity. During the development of NOTAR system, a coefficient called momentum coefficient is described which gives the relation between these properties. The momentum coefficient formula is given below [14];

$$C_\mu = 2(\rho_j/\rho_\omega)(V_j/V_\infty)^2(d_s/d_f) \tag{3.62}$$

where C_μ is momentum coefficient, ρ_j is slot jet air density, ρ_ω is wake air density, V_j is velocity of slot jet air, V_∞ is main rotor wake velocity, d_s is slot height, and d_f is boom diameter.

Using this equation 3.62 air flow velocity exits from the slots can be found by assuming incompressible flow;

$$V_8^2 = C_\mu V_\infty^2 (1/2)(d_f/d_s) \tag{3.63}$$

It is known that optimum momentum coefficient is determined approximately as 0.4 [14]. So for the hover case it can be taken as 0.4 and it varies depending on the internal boom condition.

$$C_\mu = 0.4 \frac{V_5}{V_{5hover}} \tag{3.64}$$

From the formula it can be seen that when downwash increases which means more required anti-torque, the slot velocity will also increase which will cause the increase on the anti-torque production for the same momentum coefficient. This makes system self compensating. Also with pedal controls, momentum of the air inside the boom changes, this makes difference on the anti torque force produce by the boom.

On the other hand, it is known that different flight conditions other than hover and different atmospheric conditions effect the boom torque production. The lift production varies depending on the free stream velocity value and the angle which the boom receives. In order to include these effects, some wind tunnel and flight test data obtained by MDHC during the NOTAR development is used [6].

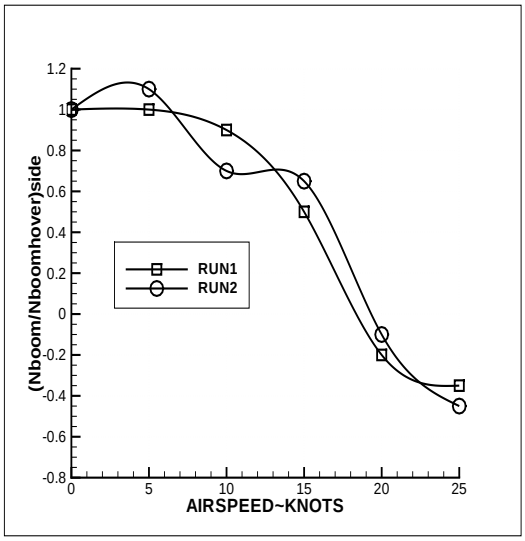

Figure 3.7: Right Flight Effect on Boom Yawing Moment [6]

The effect of the right sideward flight on the boom is determined from flight test data obtained

by MDHC. The boom yawing moment effect of the right sideward flight is normalized by yaw moment in hover which can be calculated by using the relation between the boom and direct jet thruster. This sideward flight effect is given in figure 3.7 from reference [6].

Also the effect of forward flight on boom yaw moment production is given in a graph again normalizing with the hover yawing moment. Thus the boom anti-torque production on forward flight can be found by using the relation and the values of 3.8 from reference [6].

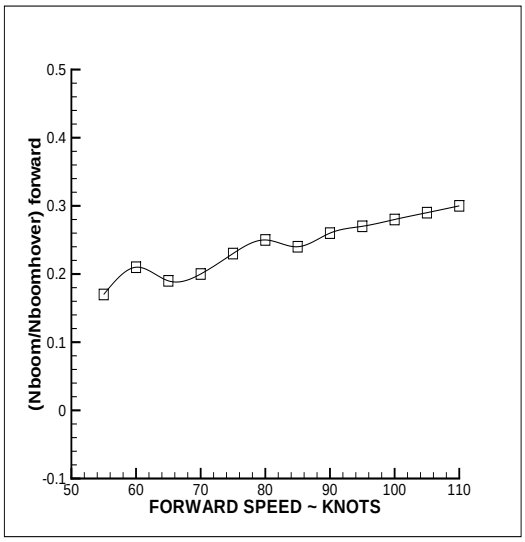

Figure 3.8: Forward Flight Effect on Boom Yawing Moment [6]

In addition, it is founded that the side force created for the anti-torque production by the boom can be concentrated on the mid section of the boom. The Pressure Instrumented Flight Test which is done by MDHC engineers in hover, low speed flight as well as in forward flight cases show that the sectional and total aerodynamic loads on the boom can be concentrated in mid section of the boom [6]. The solutions of the flight tests are given on figure 3.9

3.3 Vertical Tail Calculations

There are two vertical tails on a NOTAR model. In this NOTAR model only the left vertical tail is controlled by the pilot and the right vertical tail is controlled by the Yaw SAS system.

The angle of attack of the horizontal tail is calculated considering the real-time incidence change through pilot pedal input and real-time flight incidence yaw angle. In calculations

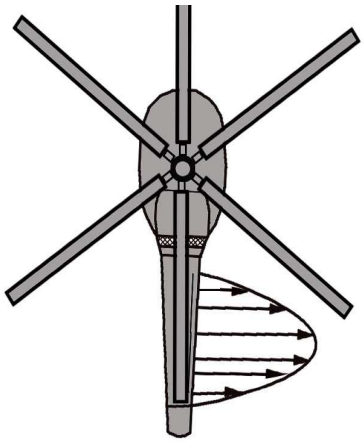

Figure 3.9: Lift Concentration on The Boom [6]

three dimensional effects are ignored since it is a simple rectangular platform with symmetrical airfoil shape.

3.4 The NOTAR Mathematical Model

Analyzing the aerodynamic solutions of each component of the NOTAR system and their relation to each other, a method is developed for a NOTAR system and based on this theory, a mathematical model is developed. In the model, solutions depends on pilot pedal input, outside air condition and flight mode of the helicopter. Looking at the aerodynamic solutions, it can be seen that when the velocity entering from the inlet V_1 is known, all other parameters can either be calculated. Therefore, the method is developed to predict V_1 together with other unknown parameters.

During the development two main assumptions are made. First assumption is that the circulation control tail boom provides nearly 60% of the required main rotor anti-torque, and the direct jet thruster produces the remaining in a hover trim flight, as it is determined in [3], [2], [6], [7], [8], [9], [10]. The second main assumption V_7 does not varies with thruster opening. Using the second assumption, it is obtained that the pressure inside the circulation lift tail boom can be assumed constant as it is stated in [3], [8], [2]. And the pressure inside the boom is between 0.5 to 1 psi above the outside air pressure.

Theory starts from the hover condition because there is enough information for the hover

case. During hover condition, there is a specific pedal position that maintains the required anti-torque by controlling the NOTAR fan pitch angle and thruster opening area. This means, there is a specific air flow rate and internal boom pressure value which produces thrust force on the direct jet thruster, and also causes a specific amount of slot exit velocity. On the other hand, it is already assumed that the circulation control tail boom provides nearly 60% of the required main rotor anti-torque, and the direct jet thruster produces the remaining in a hover trim flight. Therefore knowing the pedal position for a specific hover condition, the inlet velocity V_1 can be calculated.

When the pedal position of the helicopter changes, it changes the thruster exit area together with the NOTAR fan pitch angle. When the thruster exit area changes, the internal boom pressure leans to change. But it is known that the fan aims to keep internal boom pressure constant [3], [8], [2]. This means that the fan pitch angles change to keep the internal boom pressure constant. And this can only be done by changing the mass flow rate of the flow. Therefore there is a relation between fan pitch angle and thrust exit area. The geometrical relation between these two components are already known. Such as, when fan pitch angle changes for a given value, the change in the thruster exit area can be calculated. But in order to find the aerodynamic relation three different approaches are pursued: The approaches are; constant exit velocity, constant fan pressure ratio and constant fan blade angle of attack. At the end of the studies, the condition which both satisfies constant exit velocity and constant angle of attack approaches are found. Therefore the constant exit velocity assumption which is also satisfied for constant fan blade angle of attack assumption is selected for the model approach.

Therefore the mathematical model is developed based on these approaches.The results of the model developed depending on this approach are given in the following chapters. The approach depends on two main assumptions and all of the parameters can be calculated depending on given pedal position, outside air condition and flight mode of the helicopter.

The flow chart of the NOTAR model is given below. In this model it is assumed that the exit velocity is predicted. The modified version of this model which is developed in order to find exit velocity is also given at the end of this section.

The flow chart of the model is described in the figure 3.10. It starts with pilot pedal input.

According to the geometrical relations, the thruster exit area A_7 and no lift blade angle B_N is calculated. Although V_7 is known, in order to calculate inlet velocity V_1, slot exit velocity V_8 is needed according to the equation 3.44. Since V_8 depends on V_1, an iteration is needed. In fact nearly 10 iteration is enough to get good results. Therefore initiating V_8 is equal to zero, V_1 can be calculated. When V_1 is known, P_1 can be calculated using equation 3.1.

Using equation 3.2 and 3.7 properties on section 2 can be calculated. A loss prediction is needed depending on V_2 for inlet.

Then fan calculations start with calculating flow coefficient with equation 3.24. Then using equations 3.30, 3.31, 3.23, 3.26, 3.29, 3.28, 3.32, 3.18 respectively, all of the fan parameters can be calculated.

Using equations 3.34 and 3.35 stator properties, and using equations 3.36 and 3.37 diffuser properties can be calculated.

Then using equations 3.64 and 3.63, V_8 can be calculated. The value of V_8 is used for V_1, V_6 and circulation Γ calculations.

Using equations 3.38, 3.42, 3.43 and 3.46, thruster exit conditions are found. Then equation 3.47 gives direct jet thruster force production, thus anti torque production of direct jet thruster is calculated.

On the other side when V_8 is calculated, using the equation 3.58, circulation Γ can be calculated for a specified main rotor downwash velocity. Using circulation and equation 3.61, the anti torque production of the circulation control tail boom is calculated. The forward flight or side flight effect can be included by changing the value and direction of the downwash velocity of the main rotor.

In addition, a method for predicting the exit velocity V_7 is developed by modifying the current NOTAR model and it is given in figure 3.11. As a starting point a flight test data on hover condition can be used. When the required anti-torque is known, than the required force production from the direct jet thruster can be calculated. This can only be done by a specific exit velocity. By iteration this exit velocity can be calculated. When the exit velocity is specified once than actual NOTAR model can be used.

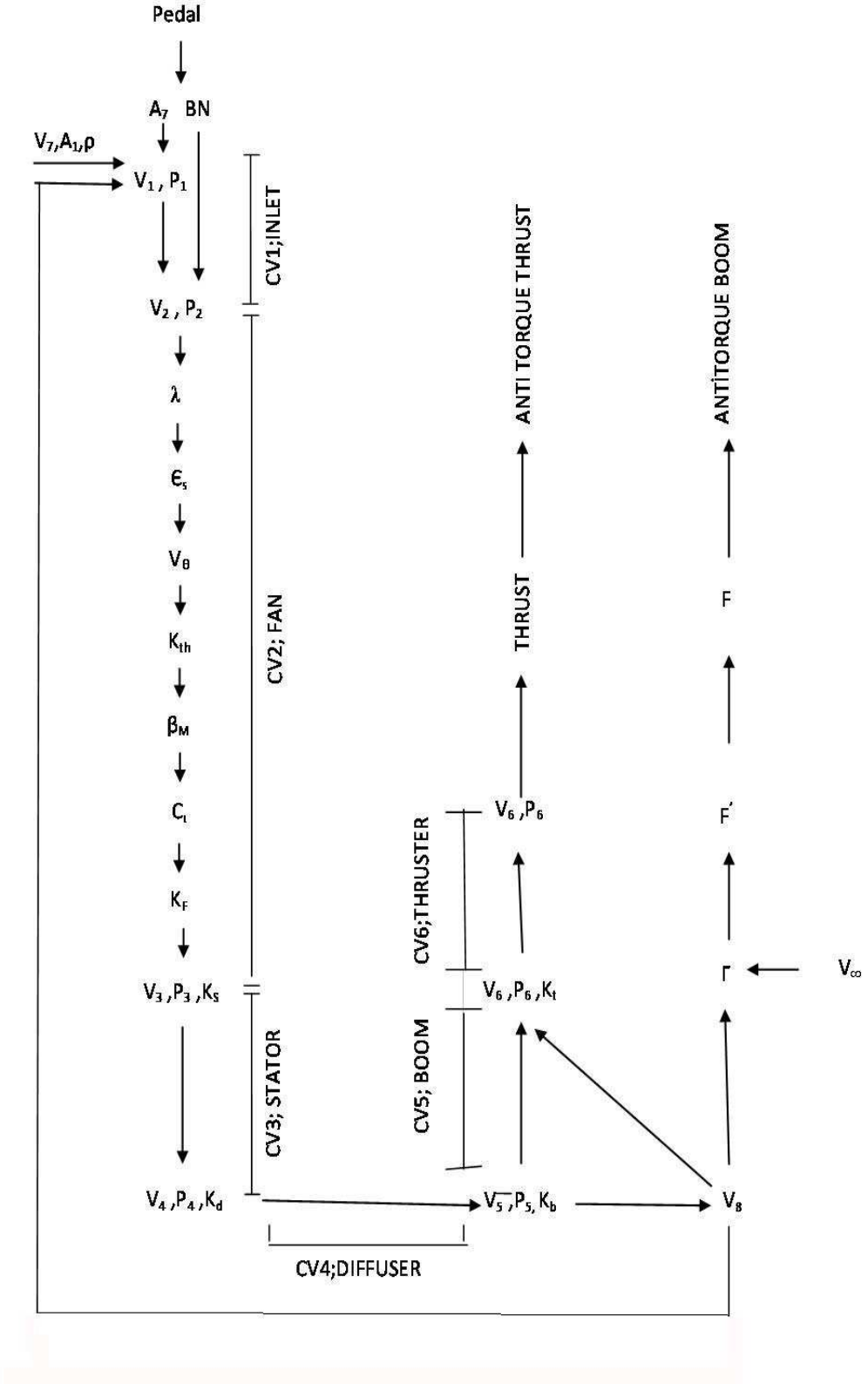

Figure 3.10: A General Schema of NOTAR Model

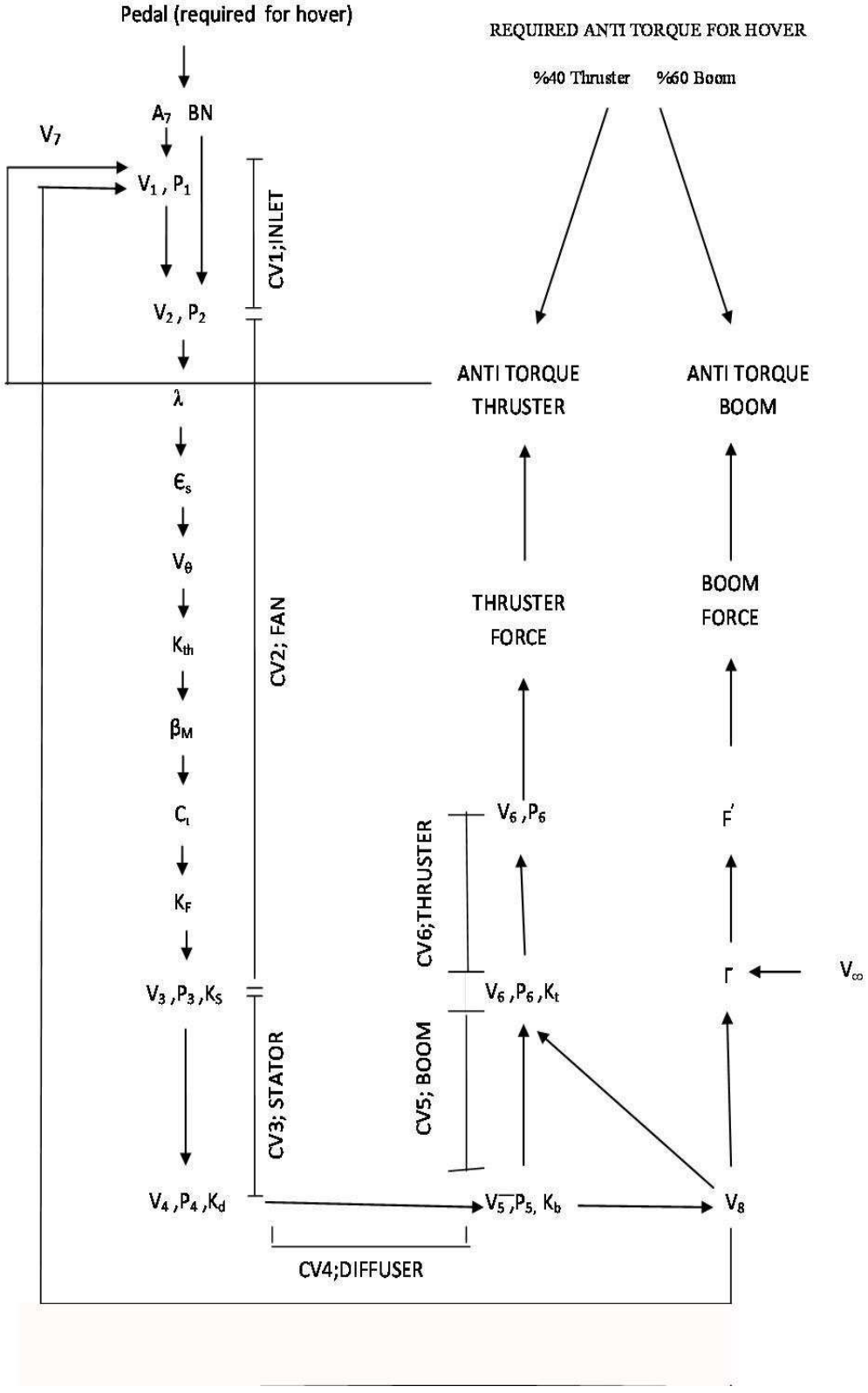

Figure 3.11: A General Schema of V7 Prediction for NOTAR Model

CHAPTER 4

MD 600N HELICOPTER FLIGHT TEST

MD 600N helicopter, which is one of the three certified NOTAR helicopter types is flight tested in order to compare and verify the developed NOTAR model. First, the helicopter is instrumented. Then flight tests are performed in a methodology developed to understand the helicopter responses to pilot inputs. Finally the data obtained from the flight test is analyzed.

4.1 MD 600N Helicopter Description

The MD 600N is a single turbine-engine multi-purpose light helicopter, which has a fully articulated six-bladed main rotor system, with anti-torque provided by a NOTAR system. The helicopter is developed by MDHC.

The helicopter is powered by a Rolls-Royce Allison 250-C47M turboshaft engine, which is derated to 600 shp for takeoff and 530 shp for maximum continuous operation. The engine is equipped with full authority digital electronic control (FADEC) [18].

Power from the engine is transmitted through the engine drive shaft to the main rotor transmission. The main rotor transmission, through a second drive shaft, drives a gear box for the NOTAR system fan. An overrunning clutch between the engine and the main rotor transmission permits freewheeling of the rotor system during autorotation [18].

The airframe is designed to provide extremely clean aerodynamic lines. This contributes to excellent handling qualities, low vibration levels and high-speed capability.

FADEC system of the 250-C47M engine enhances engine control and reduce pilot workload, improve flight safety and decrease maintenance requirements. A separate hydro-pneumatic

fuel control system is provided for manual backup in case of emergencies. The engine control unit records all important engine parameters and provides maintenance information. Also the recorded parameters can be downloaded to a personal computer.

Flight controls in the MD 600N are designed to be lightweight, simple to use and easy to maintain. Therefore it does not need the hydraulic controls. The anti-torque pedal controls the NOTAR fan pitch angles, vertical stabilizer and rotating thruster motion. Adjustable friction devices are installed in the cyclic, collective and throttle controls. In addition, electrical cyclic trim actuators are installed in order to allow flight loads to be trimmed out.

The NOTAR System on MD 600N is the same as MD 520N helicopter and it is exactly the same as it is described in Chapter 2.

The helicopter optionally has a Yaw Stability Augmentation System (Y-SAS). The system is installed on the right side vertical stabilizer. In order to correct out of trim flight, yaw rate data drives the right side vertical stabilizer. The left-side vertical stabilizer is not connected to Y-SAS system but it is connected to pilot pedal.

The MD 600N has a maximum gross weight of 4100 lb and 1700 lb of it is useful load. The helicopter has a cruising speed of 134 knots and maximum speed of 152 knots. Also the helicopter can operate at the altitude of 20000 ft and can hover in ground effect at 11000 ft.

The detailed specifications of the helicopter is given on Appendix A.

4.2 Instrumentation

During the tests, data is gathered from a Inertial Measurement Unit (IMU), sensors already installed in the helicopter, Pilot Instrument Panel, GPS Navigation Computer, Meteorology tower and wind suck. Most of the information required can be taken from sensors already present on the helicopter. In addition, the attitude information of the helicopter is taken from an IMU called Microstrain 3DM-GX1 Gyro Enhanced Orientation Sensor which is installed at the C.G of the helicopter. The pilot instrument panel is used for obtaining airspeed and as a back up for various data. GPS system is used together with the velocity indicator in the instrument panel of the helicopter so that the pilot can fly into the wind during the 60 knot flight cases. Also wind speed and direction is obtained from the meteorology tower and the

wind rose.

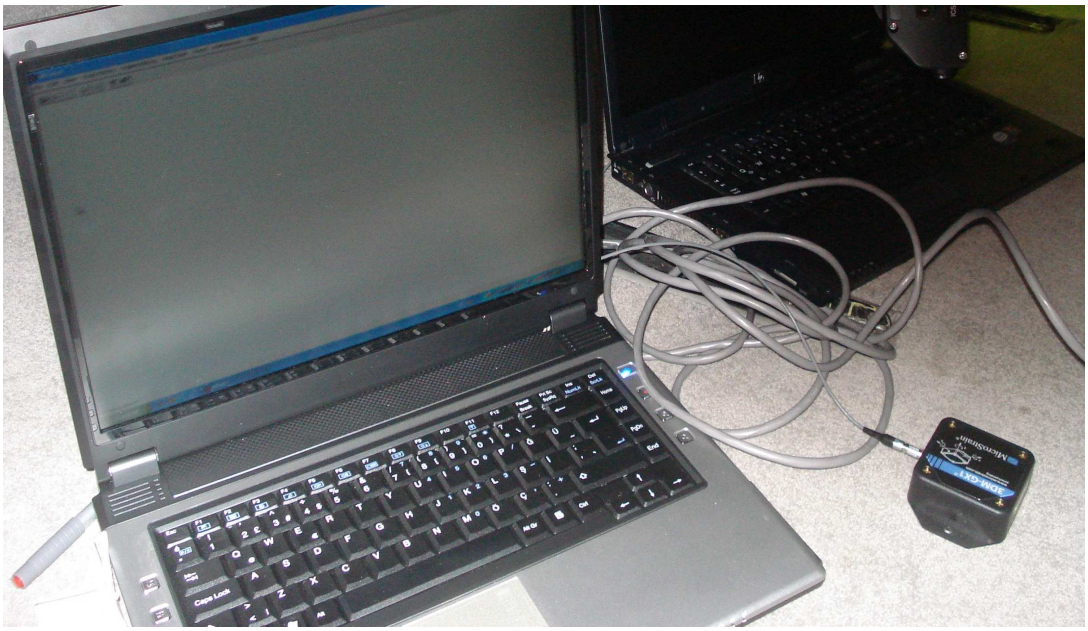

Figure 4.1: Microstrain MU 3DM-GX1 Inertial Measurement Unit

The IMU consists of three angular rate gyros with three orthogonal DC accelerometers, three orthogonal magnetometers, a multiplexer, a 16 bit A/D converter. It has also a microcontroller which outputs its orientation in dynamic and static positions. The IMU operates in 360 degree of angular motions and it can bring out the attitude of the helicopter in Euler formats. The IMU needs a computer so that to save the measurement data through a serial port. Therefore a laptop computer is used to save the data during the flight test.

4.3 Methodology

A test methodology is devised so as to understand the NOTAR effects on the helicopter anti-torque production and to compare the NOTAR concept with its model which is developed under the scope of this thesis. First of all, the required data that needs to be recorded and which required data can be obtained from which instrument are determined. Then maneuvers that need to be accomplished are also determined.

4.3.1 Test Data

The data which is required in order to study the NOTAR concept anti-torque production and so as to validate the NOTAR model developed in this thesis is determined. The weight and center of gravity (C.G.) positions are important parameters. The pedal, collective and cyclic inputs also need to be recorded. The body Euler angles and angle rates are also required to understand the responses of the helicopter to the pilot inputs. Outside air temperature and pressure are needed for the aerodynamic and performance calculations. The wind speed and its direction is needed to know the outside atmospheric conditions. Main rotor rpm, torque parameters are also important parameters affecting the calculations.

The weight of the helicopter is calculated by adding the weights of the pilots, the crew, the instruments and the fuel on the helicopter to the empty weight of the helicopter. Then, remaining fuel is recorded to calculate the final weight of the helicopter. The C.G. of the helicopter is calculated again with the information above.

The pedal and collective inputs are recorded from the potentiometers installed for engine controls. Pedal input is recorded so as to understand the response of the helicopter to pilot pedal input. The collective input is recorded to see whether the pilot keeps the collective constant or not because collective may also effect the yaw axis maneuvers. On the other hand, cyclic inputs could not be recorded but the pilot tried to keep it constant. Although it is hard for the pilot to keep cyclic input constant, its effect on yaw axis is not as much as pedal and collective controls. The data of the pedal and collective inputs are recorded as input value per maximum input value. The maximum input values are taken as hundred and the input values are recorded as input value per hundred.

The body Euler angles and body angular rates are recorded to observe the attitude of the helicopter and to understand the responses to the control inputs which are also recorded. These information are collected by the IMU which is connected to a computer. The attitude data is recorded to the computer at the same time when the remaining data is recorded to another computer. Euler angles are recorded as degree, angular rates are recorded as degree per second.

Outside air temperature and pressure is recorded for the calculations. The temperature is recorded from the meteorology tower. Also the information from temperature sensor of the

helicopter is recorded to the computer and temperature value on the pilot instrument panel is also recorded as a back up. The outside air pressure is recorded from both pressure sensor of the helicopter and from the meteorology tower.

The wind speed and direction are recorded from meteorology tower and the wind suck for the hover flight tests. During 60 knot forward flight cases the wind speed and direction is evaluated by comparing airspeed indicator and the velocity obtained from GPS navigation computer. In fact these wind speed values are approximate values.

Main rotor rpm and engine torque parameters are recorded from the engine control system. Although the main rotor torque value can not be measured, the main rotor rpm, engine torque and pedal position data is used to estimate the main rotor torque. By keeping the collective constant, the NOTAR fan power change with pedal input is observed.

4.3.2 Test Maneuvers

After the parameters required to be recorded are determined, the maneuvers that are to be performed are decided. First, tests are done from a hovering condition, then a 60 knots forward flight case is considered.

In hover tests, the pilot firstly finds the trim position into the wind and then applies the pedal control input. At the beginning; four different control inputs in four different positions and in two different places were planned. The main rotor torque should be calculated precisely in order to analyze the collective input. Only the variation in the pedal input is decided for the test.

Two different test areas are chosen for the hover tests. The two test areas have a 400 ft altitude difference and therefore pressure and temperatures are different. Also the wind condition of the two places are different. For each place, four cases are planned. First, two cases start with left pedal input and then continue with right pedal input. Second, two cases start with right pedal input and continues with left pedal input. The value and the time of the inputs vary but in any case pedal input does not take more than 15 seconds. Besides, during pedal inputs both collective and cyclic controls are kept constant by the pilot.

The 60 knot flight test cases are determined to be at an altitude of 4400 ft from mean sea level

since this is 1000 ft above the ground - a safe altitude for the test. Two cases are planned and in both cases and the flights are planned to be into the wind. The first case starts with a left pedal input and then continues with a right pedal input. Then, two cases start with right pedal input and continue with left pedal input. During these inputs, cyclic and collective are planned to be constant and the duration of the inputs are not more than 10 seconds because pedal input for a long time in an forward flight is not an advisable condition.

4.4 Flight Test

During the test flight the helicopter had a weight of 3600 lb. The helicopter empty weight was 2400 lb. Weight of two pilots and two crews with their equipment were totally 800 lb. Fuel weight at the beginning was 400 lb. The C.G. location was calculated according to this information and it was 95 in from the datum of the helicopter at the beginning. Fuel weight at the end was 180 lb; therefore total weight was 3380 lb at the end of one hour flight. And the C.G. location at the end was 97 in from the datum. The information is given on table 4.1.

Table 4.1: Weights and C.G. Locations During The Flight Test

	Begining	End
Weight	3600 lb	3400 lb
C.G	95 in	97 in

The wind condition in test area one was from east and 5 to 10 knot and the air temperature was 15 ^{o}C on that day. The Altimeter setting was recorded as 1012 mb and the pressure altitude of place one was 3700 ft.

The wind condition in test area two was approximately 3 to 6 knot during the flight. The air temperature was recorded as 16 ^{o}C and the pressure altitude was 3300 ft.

Test area three had a pressure altitude of 4400ft and the wind condition was 10 to 15 knots. This area was used for forward flight tests.

The air conditions during the flight tests are given on table 4.2.

Ten cases were measured but the best seven are taken into consideration. On the selection of these cases only the control inputs are taken into the consideration. In the selected seven, which are shown on table , pilot pedal inputs are good enough to obtain a good analyze and

Table 4.2: The Air Conditions on Test Areas

	Hover Flight Tests		60 knots Forward Flight Tests
Test Area	Area 1	Area 2	Area 3
Pressure Altitude	3700 ft	3300 ft	4400ft
Wind	5-10 knots	3-6 knots	10-15 knots
Temperature	15 ^{o}C	16 ^{o}C	14 ^{o}C

the pilot collective inputs are nearly constant at the same time.

Table 4.3: Flight Test Cases

CASE	Flight Condition	Test Area	First Pedal Input	Second Pedal Input
1	Hover	1	Left (%3)	Right (%9)
2	Hover	2	Left (%9)	Right (%5)
3	Hover	1	Left (%7)	Right (%14)
4	Hover	1	Right (%13)	Left (%22)
5	Hover	2	Right (%3)	Left (%12)
6	Fwd Flight	3	Left (%12)	Right (%5)
7	Fwd Flight	3	Right (%4)	Left (%9)

4.4.1 Case 1

The test flight case one was obtained on test area one. Here, the pilot kept hover trim position into the wind for a while and then applied left pedal input. After some time pilot applied right pedal input. At the same time, the pilot kept collective input constant. Although it is hard to keep cyclic constant during a hover, the pilot tried to keep it fixed as much as possible.

During the flight test case one, the wind was 5 knot from the east. Temperature was 16 ^{o}C and pressure altitude was 3700 ft. The helicopter weight was approximately 3500 lb and the C.G. was calculated as 96 in.

4.4.2 Case 2

In case two, the pilot applied the inputs in the same way as case one but in different magnitudes. Also, case two was done in test area two, where atmospheric conditions were different.

During the flight test case two, the wind was 6 knot from the north. Temperature was 17 ^{o}C and pressure altitude was 3300 ft. The helicopter weight was approximately 3500 lb and the

C.G. was calculated as 96 in.

4.4.3 Case 3

In case three the pilot again applied left input at first but did not keep trim position for a while and kept left pedal inputs approximately 3 seconds which means nearly double amount of time. It was done in place one but it was a high wind condition.

During the flight test case one, the wind was 5 to 10 knots from the east. Temperature was 16 ^{o}C and pressure altitude was 3700 ft. The helicopter weight was approximately 3600 lb and the C.G was calculated as 95 in from datum.

4.4.4 Case 4

In case 4 the pilot applied right pedal input from the hover trim position into the wind. After some seconds he applied left pedal input and again he kept collective and cyclic inputs constant. This test was done in test area one.

During the flight test case four, the wind was 5 to 10 knots from the east. Temperature was 16 ^{o}C and pressure altitude was 3700 ft. The helicopter weight was approximately 3600 lb and the C.G. was calculated as 95 in.

4.4.5 Case 5

In this case the pilot firstly kept trim position for a while and then he applied right pedal input but in lower magnitudes and less amount of time. Then he applied left pedal for some time and then right pedal again. The case one was done in test area two.

During the flight test case five, the wind was 6 knots from the north. Temperature was 17 ^{o}C and pressure altitude was 3300 ft. The helicopter weight was approximately 3500 lb and the C.G. was calculated as 96 in.

4.4.6 Case 6

In this case the pilot firstly kept trim position in 60 knots forward flight for a while and then applied left pedal input. Then he applied right pedal input for some time. The case six was done at 4400 ft pressure altitude.

During the flight test case six, the wind was approximately 10 knots from the north. Temperature was 14 ^{o}C. The helicopter weight was approximately 3500 lb and the C.G. was calculated as 96 in.

4.4.7 Case 7

In this case the pilot firstly kept trim position for a while in 60 knots into the wind and then he applied right pedal input for a while and then applied left pedal input. The test case seven is also done also at 4400 ft pressure altitude.

During the flight test case six, the wind was approximately 10 knots from the north. Temperature was 14 ^{o}C. The helicopter weight was approximately 3500 lb and the C.G. was calculated as 96 in.

CHAPTER 5

NOTAR MODEL VERIFICATION

The NOTAR model described in section 3 is integrated to a simulation math model program based on the minimum complexity helicopter theory [12]. Applying the same pilot pedal inputs used in test flight the response of the model is compared with flight test data. The comparisons showed promising results and therefore the approach is thought to be adequate for simulation purposes.

5.1 Integration to the Simulation Program Based On the Minimum Complexity Model

The developed NOTAR model is integrated into the minimum complexity helicopter simulation math model program. At first, tail rotor calculations of the simulation are replaced with the developed NOTAR model. Then the program is modified for the MD 600N helicopter and its properties are included. Unknown physical properties of the helicopter are found by measurement or comparison to similar helicopters. Finally, the vertical tail model is updated since the minimum complexity vertical tail model was not good enough for a NOTAR model.

In the minimum complexity theory [11], the helicopter is modeled as simple as possible so that it can assure enough effective handling qualities for piloted simulation. Therefore, the theory aims to calculate only the effects that can be felt by a pilot. Therefore, many component models are simplified. For example, first order flapping dynamics is used for the main rotor flapping calculations. Induced velocities of the both main and tail rotors are calculated with iterative methods based on classic momentum theory and Glauert theory and inflow model is assumed to be uniform. For NOTAR model a program based on this theory is used but tail ro-

tor calculations of minimum complexity theory are changed and NOTAR model calculations are integrated. Also vertical tail calculations are updated.

Properties of MD 600N helicopter are included into the program. Since the helicopter has a six bladed fully articulated main rotor, some modifications are needed to be done on the original program. Properties that could not be found in references are determined by examining, measuring and approximating. For example, the main rotor airfoil is estimated by examining the shape of it. Also some properties like effective hinge offset or strap packs used for flapping are approximated. The inertias of the helicopter could not be found and UH1-H helicopter inertias are scaled considering the weight and geometric differences of these two helicopters.

Properties for the NOTAR model itself are also found in a similar way. For example, all of the lengths and areas on the tail boom which are used in the model are measured from the helicopter. And NOTAR fan properties are estimated according to these measurements. In addition to these, the two important parameters of the model, Thruster exit area A_7 and NOTAR fan pitch angles which are variable depending on the pilot pedal are observed and measured and as a result the geometrical relations are found based on these measurement.

On the other hand, at first the vertical tail was modeled according to the minimum complexity theory. However during 60 knots forward flight velocity condition, it is observed that it caused oscillations. Therefore the vertical tail model is updated according to the updated model developed in the thesis [12], which is based on simple aerodynamic approach that uses airfoil properties calculating the angle of attack and incidence angle. The dependency of the vertical tail to the pilot pedal is also included to the model.

5.2 Comparison of the NOTAR Model with Flight Test Data

Simulation of the NOTAR Model integrated to the minimum complexity theory is compared with the flight tests performed with an MD 600N NOTAR helicopter. First of all, hover trim values are found and then several different pilot pedal input responses of the model in hover are compared with the MD 600N flight test data. The results are given below.

The responses to the pedal inputs of the model are compared with the MD 600N flight test data which is obtained by applying the same pilot pedal inputs. During the tests, the pilot

firstly tried to stay on trim conditions and then apply different pedal inputs for each trimmed flight case. Pedal input values and the responses of the helicopter are recorded. Simulation program of the model is also run for each case. The program finds the trim conditions and required pedal positions to the trimmed simulation model. Then various pilot inputs which are the same with the flight test cases are applied to the simulation models in the trimmed condition. The responses of the model are saved and compared with the flight test data.

Results are shown in the following figures: Pilot pedal input figures (5.1, 5.9, 5.14, 5.19, 5.24, 5.29, 5.34) show the applied pilot pedal inputs during the flight test on trim condition. In figures, difference between maximum left and maximum right pedal is considered as hundred units and the values are given in pedal input per hundred. The same value of pedal input is applied to the model. Pilot collective inputs during the test are given in pilot collective input figures (5.2a, 5.10a, 5.15a, 5.20a, 5.25a, 5.30a, 5.35a). The torque change of the engine because of the pedal inputs are given in engine torque figures (5.2b, 5.10b, 5.15b, 5.20b, 5.25b, 5.30b, 5.35b).

The responses of the helicopter to the pedal inputs are compared with the model responses in all three axis. Euler angle changes and angle rate changes from the trim conditions of both flight test and model are given. The angle changes are given in degree and angle rate changes are given in degree per second.

Seven different pedal inputs are applied during the flight tests and the same inputs are applied to the simulation model. Results are given on the following figures (5.1-5.38).

5.3 Case 1

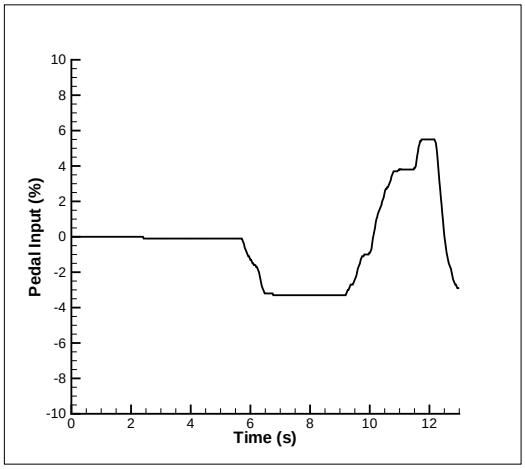

Figure 5.1: Pilot Pedal Input in Case 1.

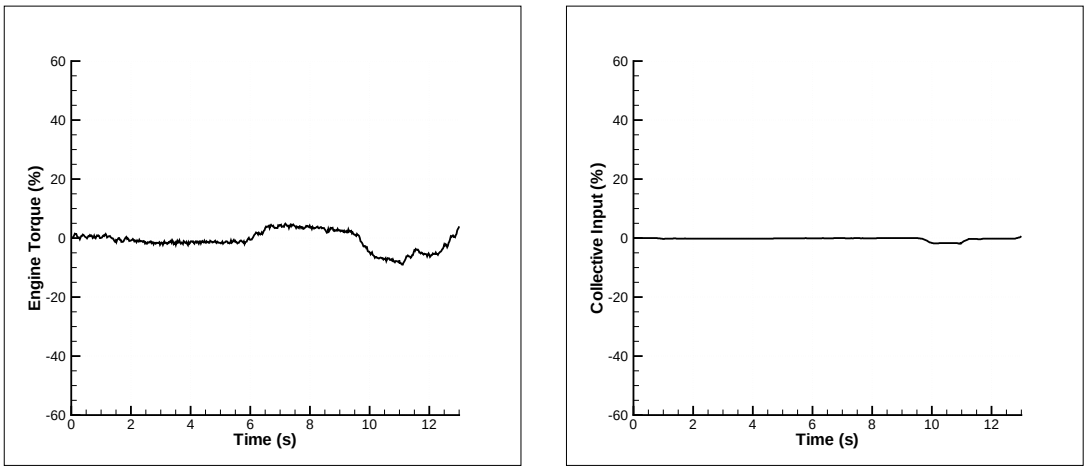

(a) (b)

Figure 5.2: Engine Torque Change and Pilot Collective Input in Case 1.

(a) Engine Torque (b) Pilot Collective Input

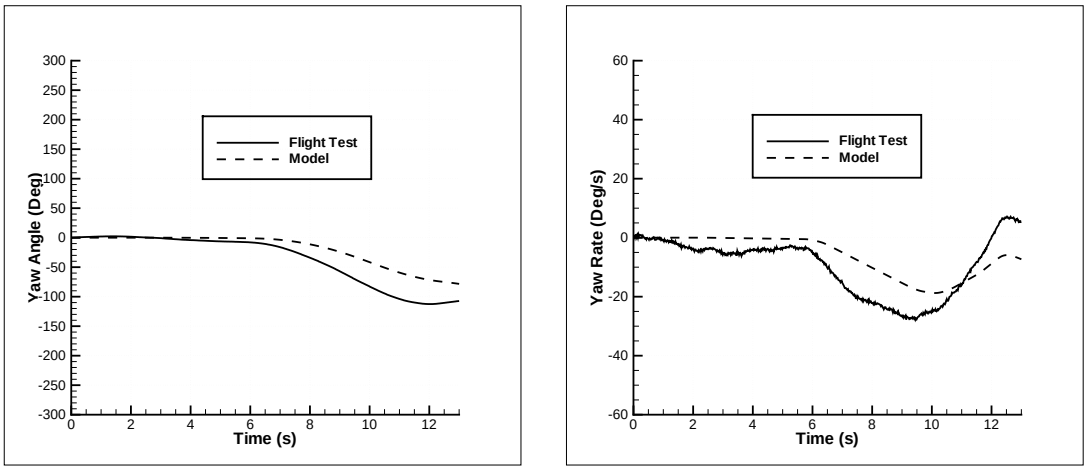

(a) (b)

Figure 5.3: Yaw Axis Response Comparison to the Pilot Pedal Input in Case 1.

(a) Yaw Angle Response Comparison (b) Yaw Rate Response Comparison

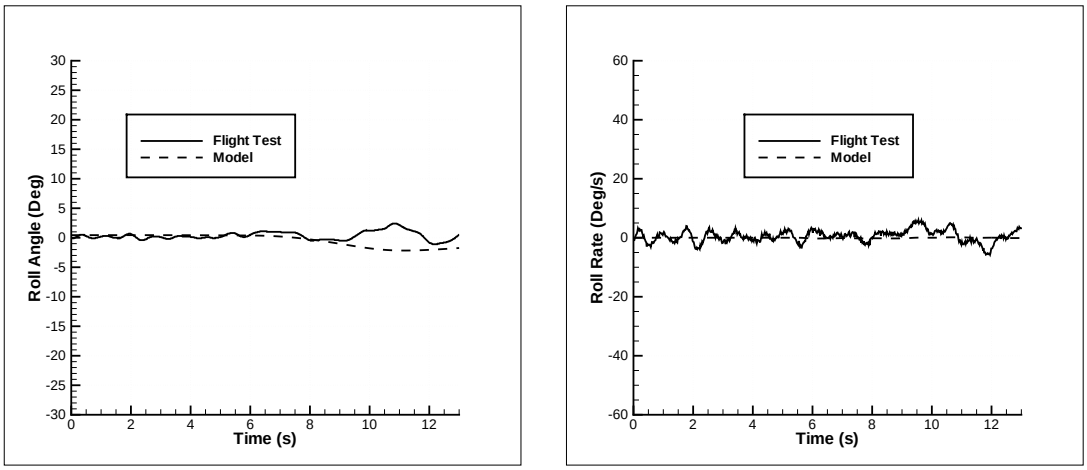

(a) (b)

Figure 5.4: Roll Axis Response Comparison to the Pilot Pedal Input in Case 1.

(a) Roll Angle Response Comparison
(b) Roll Rate Response Comparison

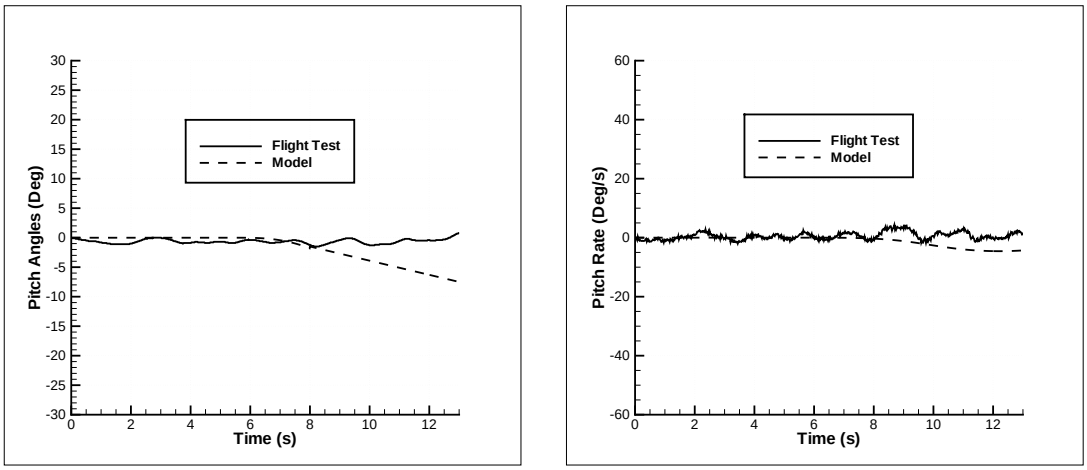

(a) (b)

Figure 5.5: Pitch Axis Response Comparison to the Pilot Pedal Input in Case 1.

(a) Pitch Angle Response Comparison (b) Pitch Rate Response Comparison

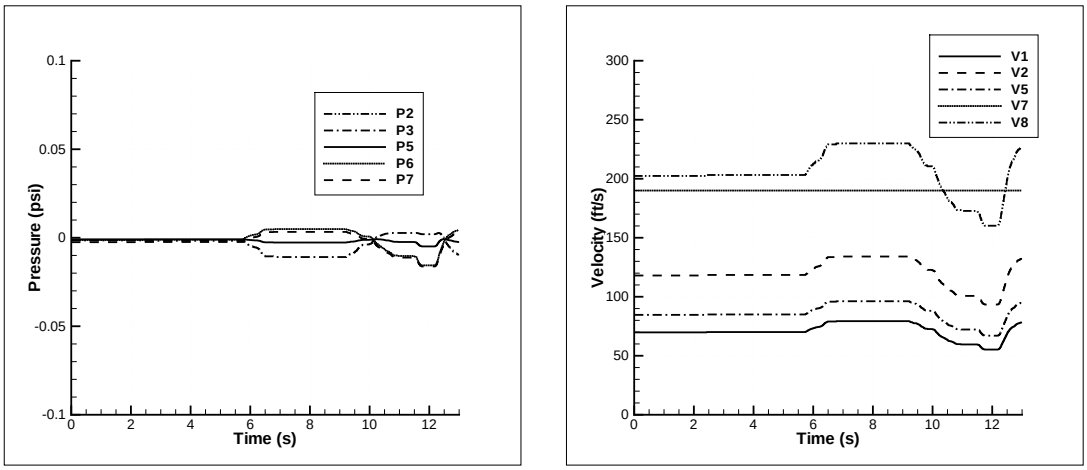

(a) (b)

Figure 5.6: Pressure and Velocity Responses to the Pilot Pedal Input in Case 1.

(a) Pressures on Different Sections (b) Velocities on Different Sections

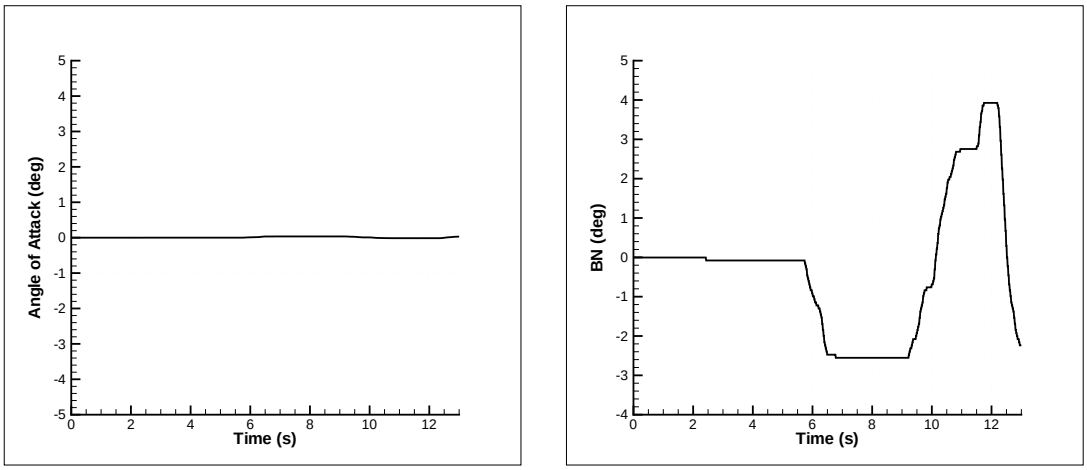

(a) (b)

Figure 5.7: Angle of Attack and BN Comparison to the Pilot Pedal Input in Case 1.

(a) Angle of Attack Response to the Pilot Pedal Input
(b) BN Values of the Pedal Input

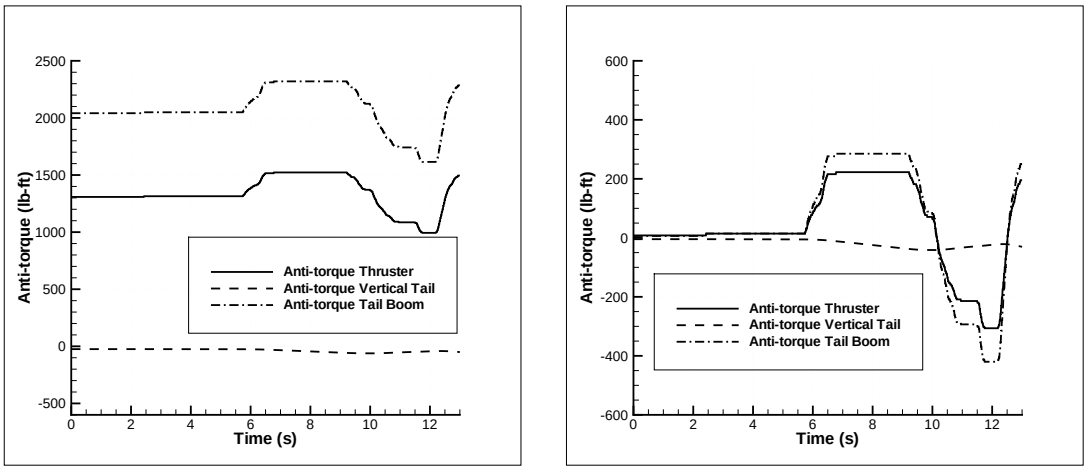

(a) (b)

Figure 5.8: Anti-torque Response to the Pilot Pedal Input in Case 1.

(a) Anti-torque Production (b) Anti-torqu Production Change from Hover

Regarding figure 5.1, it is seen that pilot keeps hover trim position for approximately 6 seconds and than applies left pedal for 1.5 seconds. Then he applies right pedal but in a greater value. The pilot tries not to give any collective or cyclic input. Is is clear from figure 5.2, the pilot keeps constant collective pitch. But cyclic values are not recorded and it is known that keeping cyclic stable is not easy during hover and this might have caused some errors, since the model works on ideal conditions and no cyclic input is given during this model calculations.

Figure 5.2, shows the pedal effects on the engine torque. Since there is no collective input, the only reason for engine torque change is pedal input. From this figure, it can be seen that when the left pedal is applied a higher NOTAR fan pitch angle, therefore more power is required. This is in contrast with the right pedal input.

As for the yaw angle and the yaw rate figures 5.3 the model responses to pedal inputs are close to responses of flight test results. This shows that the NOTAR model responses are in reasonable levels on the yaw axis. In fact, the left pedal response of the model are a little slower than the flight test and also right pedal responses of the model is slower than the flight test result. This is an expected situation because the developed NOTAR model has a symmetrical response. But in reality, a helicopter which has counterclockwise rotating main rotor, responses to the right pedal is faster than it does to the left pedal.

The error on the yaw axis also depends on the circulation control tail boom calculations. The calculations were simplified. Second, since the downwash velocity of the main rotor is used on the circulation flow calculations, the inflow model of the main rotor is important for the NOTAR model. However, the inflow model of the simulation program is not precise enough. Also, the wind is effecting the tail boom lift production and may cause some error.

As it is seen in the roll axis flight test data in figure 5.4 it is hard to stay in hover without any roll rate. Only the average value can be zero especially in windy conditions. But since the model works with less disturbance roll rate can be close to zero. In fact, considering the complete flight, the average roll rate and roll angle of the helicopter is close to zero in both model and the test flight.

Pitch axis figure 5.5 show that the error between the flight test and the simulation result is high after 6 seconds. The other reason of this error may be the fuselage model of the MD 600N helicopter, which is developed considering mostly the yaw axis. The pitch axis of the fuselage may not be modeled good enough.

The figure 5.7b shows that when pedal is applied, axial flow fan pitch angles also change. On the other hand, figure 5.7a shows that the angle of attack of the fan blades do not vary with pedal. The reason of that interesting condition is that when the pitch angle of the fan blades change, at the same time direct jet thruster exit area changes which also changes airflow rate. There is a relation between fan pitches and thruster exit area that cause this airflow rate change

to be in a manner that the angle of attack is kept constant. This condition is obtained when it is assumed that exit velocity of thruster is constant.

Interesting results are obtained in figure 5.6 and 5.7. As it can be seen from the figure 5.7a, angle of attack does not change with pedal input. Since the airflow rate changes, the pressure ratio of the fan also changes, which can be observed from P_3 on figure 5.6a. But after the stators and diffuser this pressure difference is turned into axial flow velocity 5.6b. This can be observed from 5.6a. The internal boom pressure P_5 is constant no matter what the pedal value it is.

Looking to figure 5.8, it is observed that most of the anti-torque is produced by circulation control tail boom, which is expected. Direct jet thruster produces less anti-torque when it is compared with tail boom. It is also seen that vertical stabilizer has little effect on anti-torque production during hover flight.

5.4 Case 2

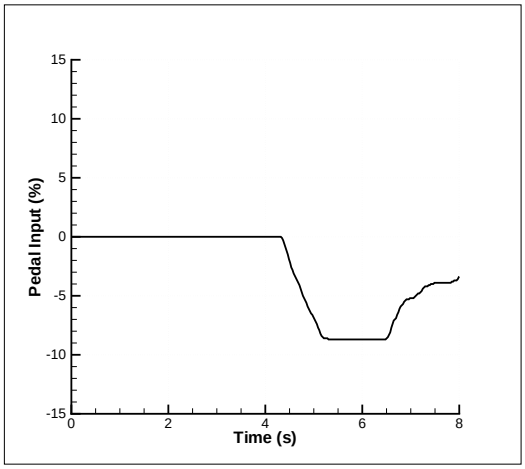

Figure 5.9: Pilot Pedal Input in Case 2.

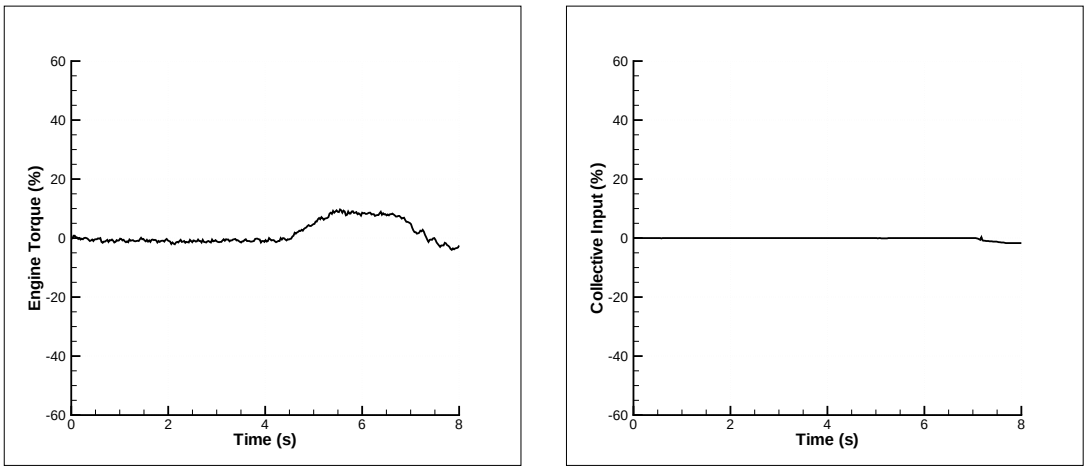

(a) (b)

Figure 5.10: Engine Torque Change and Pilot Collective Input in Case 2.

(a) Engine Torque (b) Pilot Collective Input

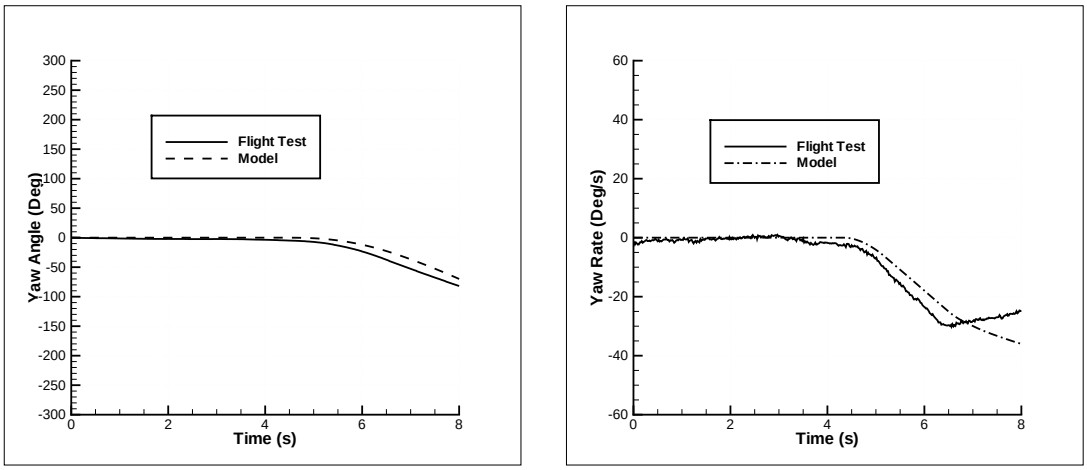

(a) (b)

Figure 5.11: Yaw Axis Response Comparison to the Pilot Pedal Input in Case 2.

(a) Yaw Angle Response Comparison (b) Yaw Rate Response Comparison

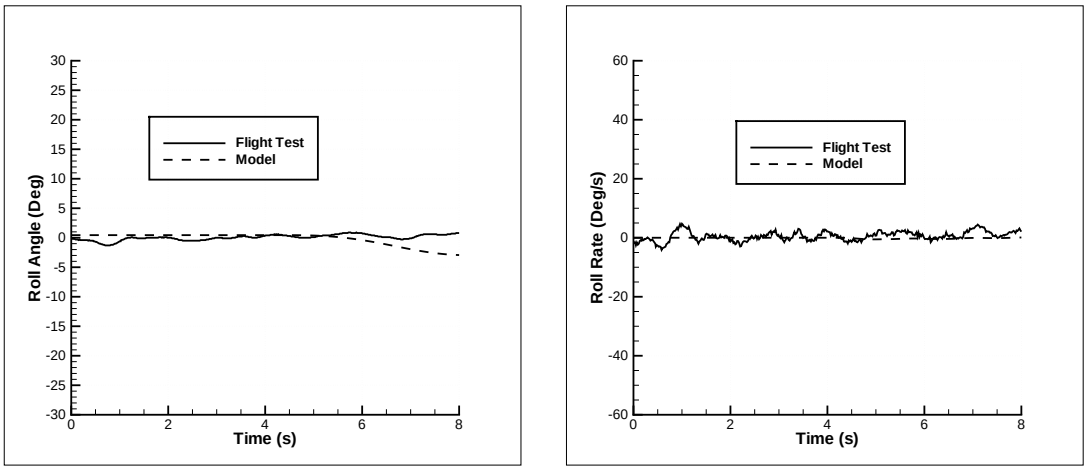

(a) (b)

Figure 5.12: Roll Axis Response Comparison to the Pilot Pedal Input in Case 2.

(a) Roll Angle Response Comparison (b) Roll Rate Response Comparison

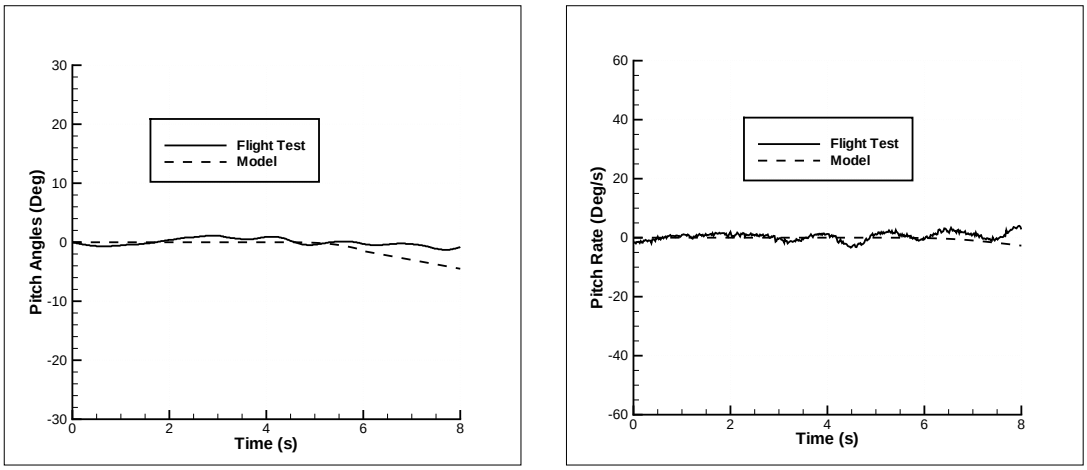

(a) (b)

Figure 5.13: Pitch Axis Response Comparison to the Pilot Pedal Input in Case 2.
(a) Pitch Angle Response Comparison (b) Pitch Rate Response Comparison

From figure 5.9 it is seen that the pilot keeps hover trim position approximately for 3 seconds and than applies left pedal for 1.5 seconds. Furthermore he applies right pedal again a greater value but in a slower manner. The pilot tries not to give any collective or cyclic input. And as it is seen that he keeps the collective constant. The flight test data was taken from a different place where the altitude is 400 ft lower and the wind is a little lower than the previous case. This atmospheric conditions are also applied to the model.

Regarding the yaw angle and yaw rate figures 5.11, it can be seen that model responses is very close to the flight test responses in that case. It seems that body yaw angle change is matched in a nearly perfect manner. In flight tests, it can be observed that right pedal response is higher when it is compared with the model pedal response. Also there is sharp rotation by the helicopter in the last two seconds of the yaw rate figure 5.11 b and is not captured in the model results. This error is most probably from the error on the wind measurement during the flight test and the prediction of the wind effect on the model. Because after applied left pedal the helicopter turns left and the wind starts coming from the right. Wind from the right hand side of the helicopter means lower boom anti-torque production and torque production from the vertical stabilizers. There are some inaccuracies in pitch and roll axis. The main reason of that error is due to the helicopter simulation program and off-axis models not the NOTAR model. When the simulation program is improved keeping the NOTAR model the same, this error should be eliminated.

5.5 Case 3

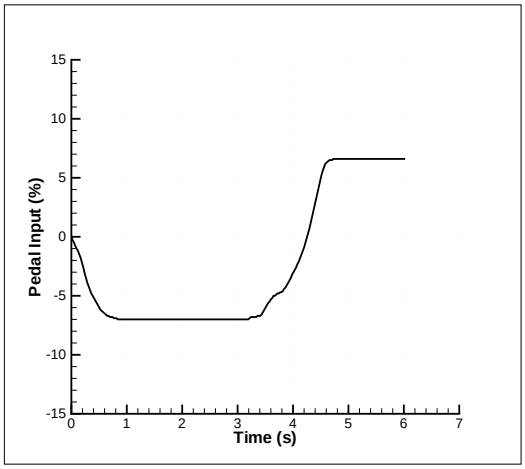

Figure 5.14: Pilot Pedal Input in Case 3.

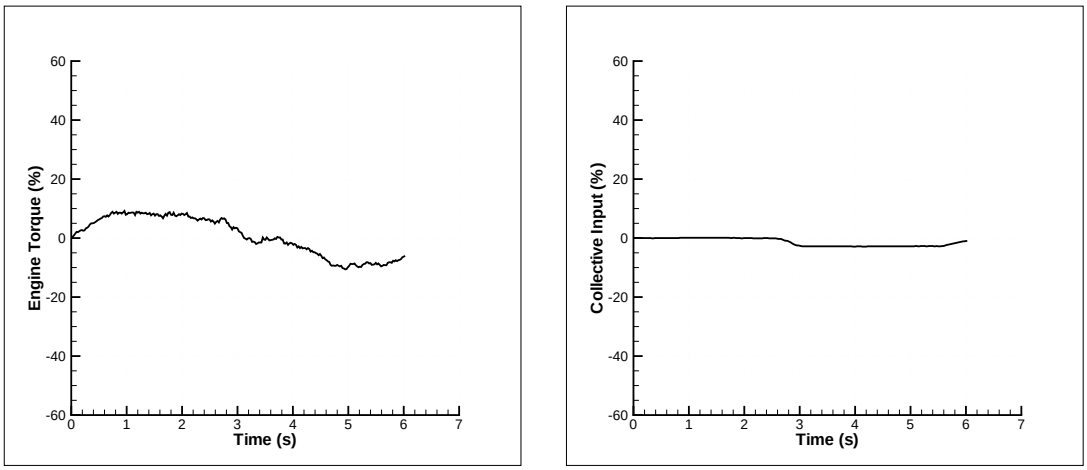

(a) (b)

Figure 5.15: Engine Torque Change and Pilot Collective Input in Case 3.

(a) Engine Torque (b) Pilot Collective Input

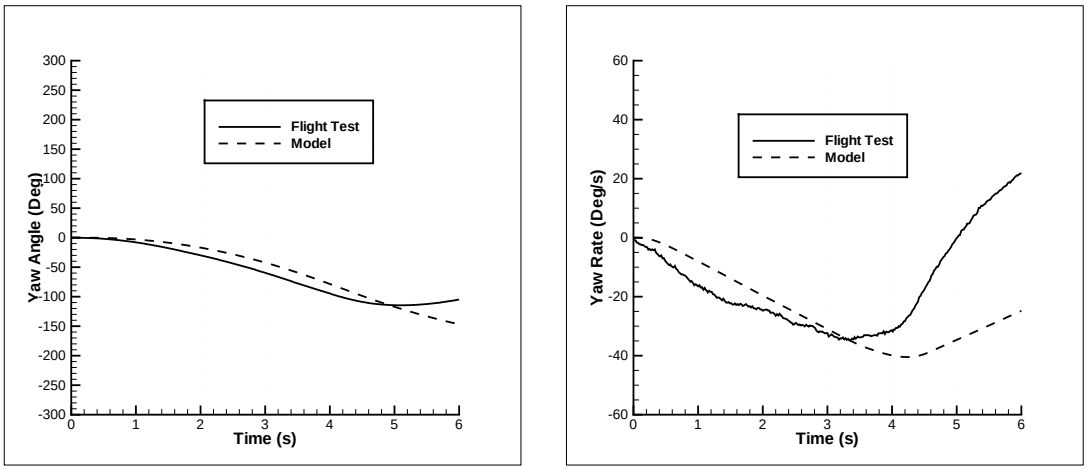

(a) (b)

Figure 5.16: Yaw Axis Response Comparison to the Pilot Pedal Input in Case 3.

(a) Yaw Angle Response Comparison (b) Yaw Rate Response Comparison

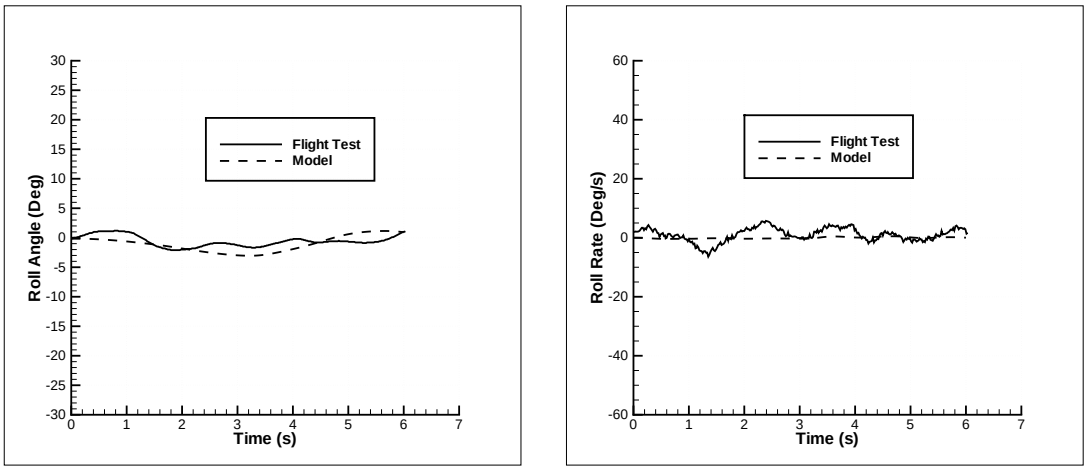

(a) (b)

Figure 5.17: Roll Axis Response Comparison to the Pilot Pedal Input in Case 3.

(a) Roll Angle Response Comparison (b) Roll Rate Response Comparison

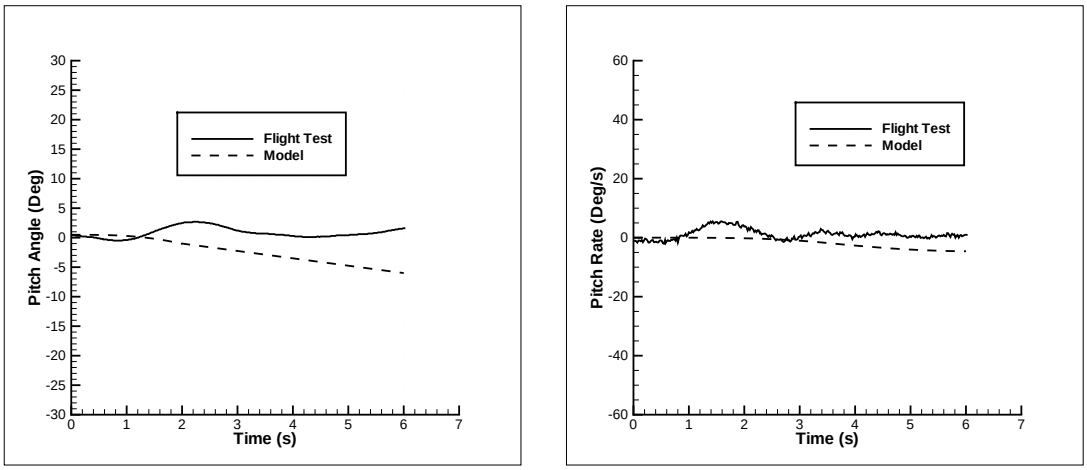

(a) (b)

Figure 5.18: Pitch Axis Response Comparison to the Pilot Pedal Input in Case 3.
(a) Pitch Angle Response Comparison (b) Pitch Rate Response Comparison

This time the pilot applies left pedal longer, approximately 3 seconds and than applies equal amount but in the opposite direction (figure 5.14). Yaw angle response is again nearly equal. But just like in previous cases the right pedal response of the model is a little low especially after the helicopter has turned more than 90 degree (figure 5.16). Also while in roll axis the solutions are on reasonable levels but on pitch axis the model solution diverges.

5.6 Case 4

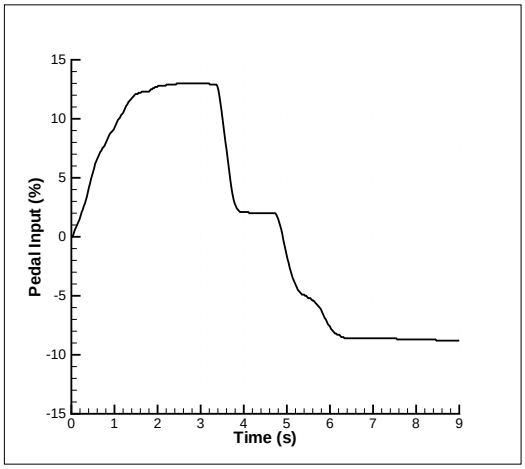

Figure 5.19: Pilot Pedal Input in Case 4.

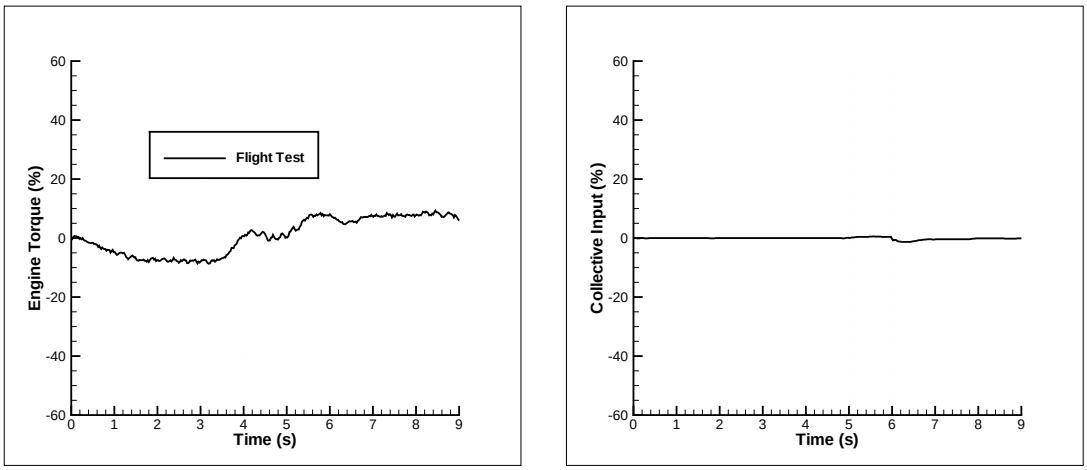

(a) (b)

Figure 5.20: Engine Torque Change and Pilot Collective Input in Case 4.

(a) Engine Torque (b) Pilot Collective Input

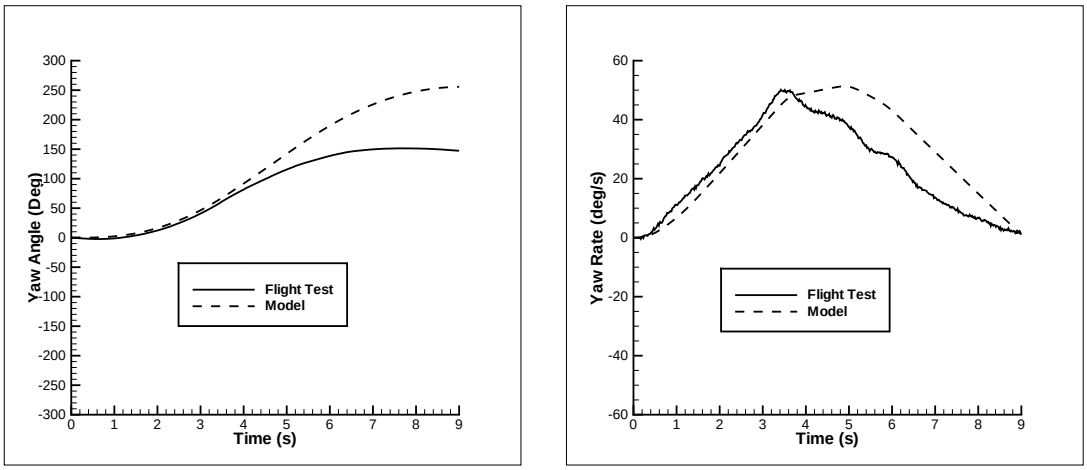

(a) (b)

Figure 5.21: Yaw Axis Response Comparison to the Pilot Pedal Input in Case 4.

(a) Yaw Angle Response Comparison (b) Yaw Rate Response Comparison

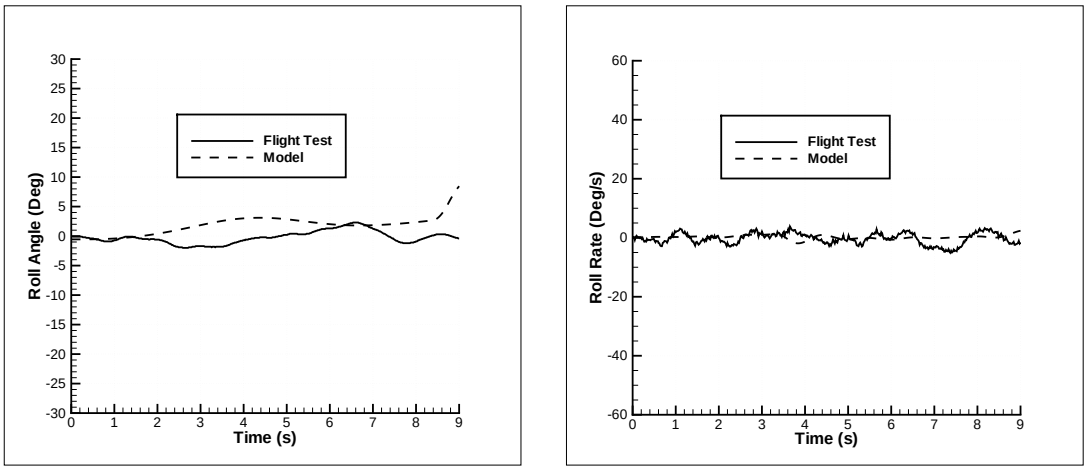

(a) (b)

Figure 5.22: Roll Axis Response Comparison to the Pilot Pedal Input in Case 4.

(a) Roll Angle Response Comparison (b) Roll Rate Response Comparison

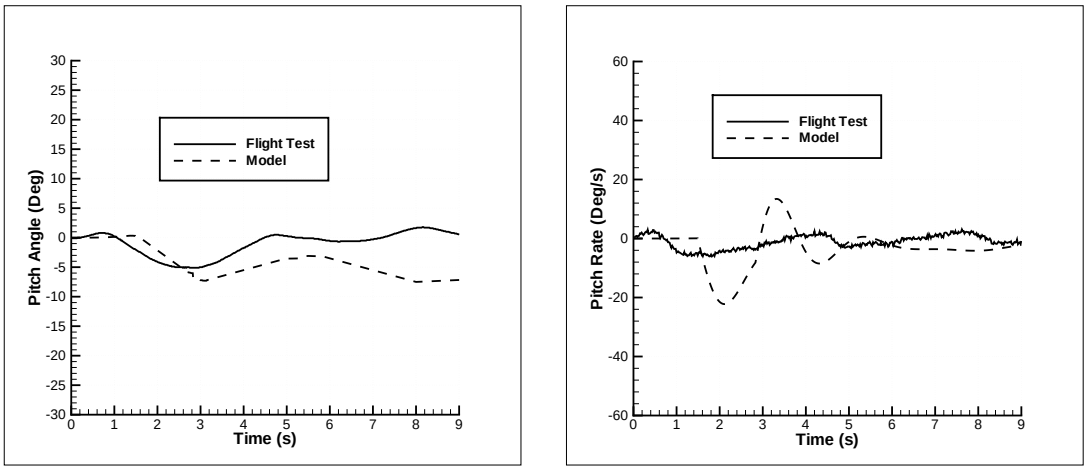

(a) (b)

Figure 5.23: Pitch Axis Response Comparison to the Pilot Pedal Input in Case 4.
(a) Pitch Angle Response Comparison (b) Pitch Rate Response Comparison

In this case the pilot applies right pedal at first and then applies left pedal. This time the value of the pedal input is a little high. Again pilot collective control is nearly perfect.

Analyzing the yaw axis response 5.21, the right pedal response of the model is close to the flight test response. But the left pedal response of the model is lower than the real flight one. The reason of the delay is again most probably because of the wind. When right pedal is applied the helicopter turns more than 90 degree right. At this position winds tends to turn the helicopter back to the left because of the vertical stabilizer and the decrease of the anti-torque production on the boom. The wind during the flight test might be more than the predicted value. Because the wind was not constant during the flight tests and the wind might have been more than 5 knot during the 4th case flight test data were taken. Also the vertical stabilizer model might not be as good or the effect of right wind to the circulation control tail boom might not be modeled well enough. Therefore, although in flight tests the helicopter tends to turn left when it is right angle to the wind, the model response is a little slow.

5.7 Case 5

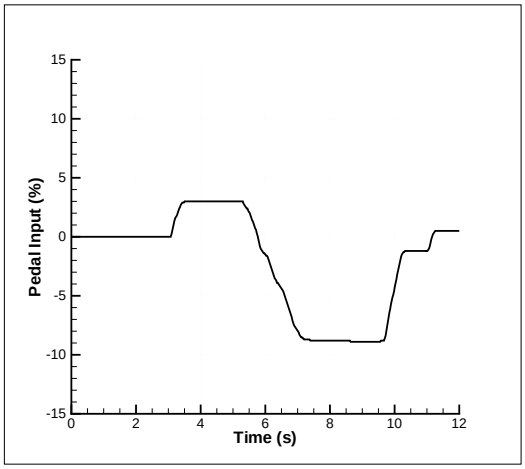

Figure 5.24: Pilot Pedal Input in Case 5.

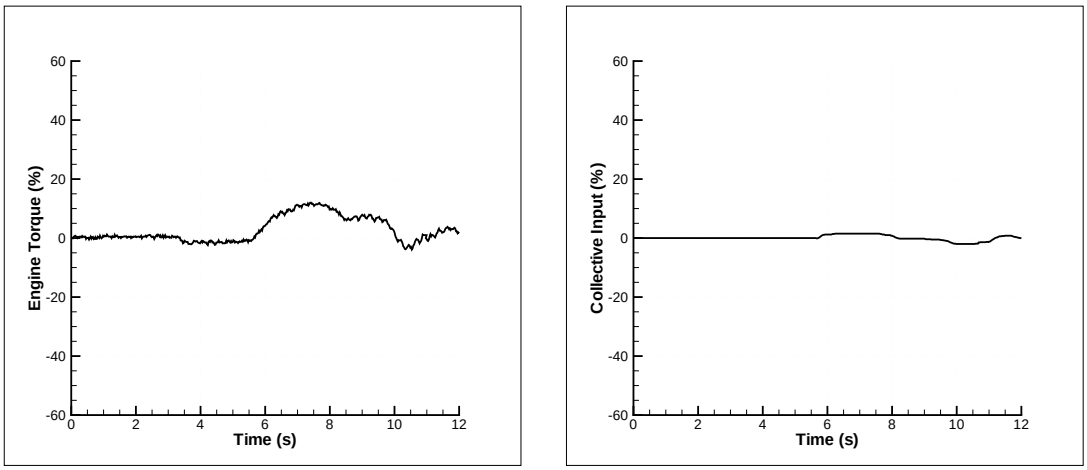

(a) (b)

Figure 5.25: Engine Torque Change and Pilot Collective Input in Case 5.

(a) Engine Torque (b) Pilot Collective Input

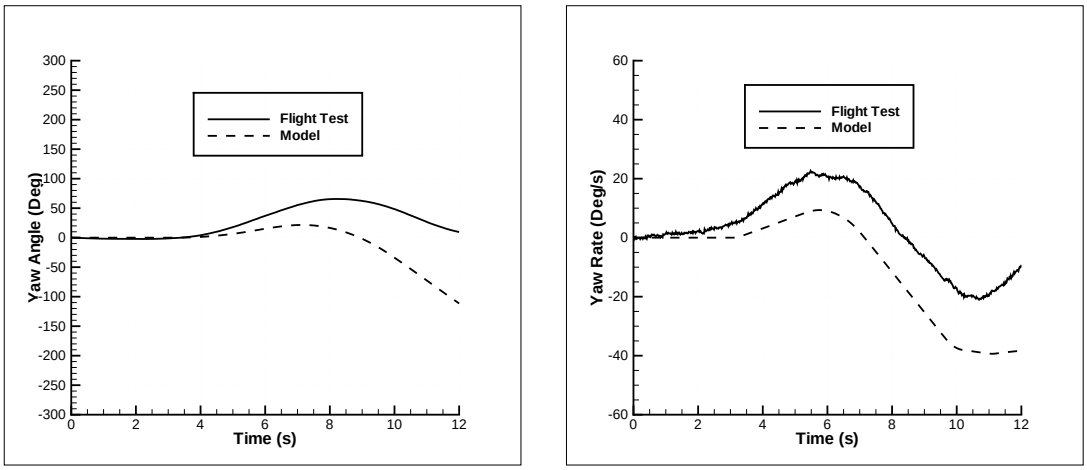

(a) (b)

Figure 5.26: Yaw Axis Response Comparison to the Pilot Pedal Input in Case 5.

(a) Yaw Angle Response Comparison (b) Yaw Rate Response Comparison

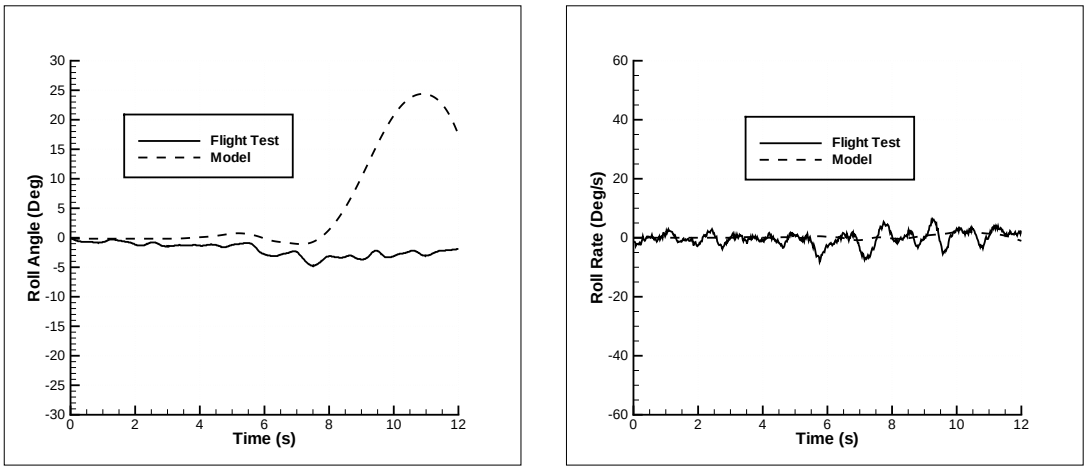

(a) (b)

Figure 5.27: Roll Axis Response Comparison to the Pilot Pedal Input in Case 5.

(a) Roll Angle Response Comparison (b) Roll Rate Response Comparison

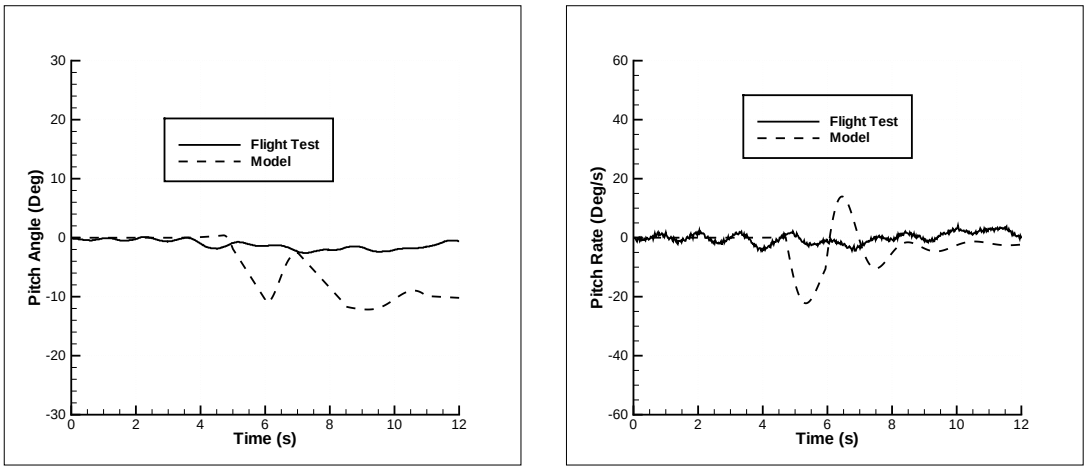

(a) (b)

Figure 5.28: Pitch Axis Response Comparison to the Pilot Pedal Input in Case 5.
(a) Pitch Angle Response Comparison (b) Pitch Rate Response Comparison

In this case, the pilot applies a small right pedal input and than a bigger left pedal input and then again a right pedal input. As in the previous cases, the right pedal response is a little less. But although left pedal response is similar, the yaw angle of the model can not catch the flight test value. On the other hand, although the right pedal response is expected to be lower, it is not expected as much as in figure 5.26. The reason of the large error on the angle is guessed as due to the pilot and the change in wind conditions during the tests. Because on the test area, it is hard to the see wind suck which shows the wind direction. Therefore the pilot might have thought that the helicopter is in trim condition into the wind but in reality, the helicopter might not be directly into the wind. Therefore the test data may be not perfect. Errors in roll and pitch axis may also cause this error.

As it is seen on the figure 5.27 and 5.28, there are large errors after 6 seconds in roll angle and divergence in pitch angle. These are not because of the NOTAR model but the simulation program which depends on the minimum complexity theory depends on the properties of the helicopter. In fact rate responses of the minimum complexity model are reasonable levels as seen from the graphs.

5.8 Case 6

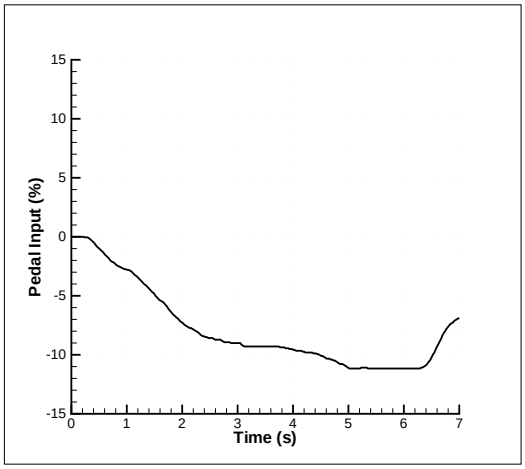

Figure 5.29: Pilot Pedal Input in Case 6.

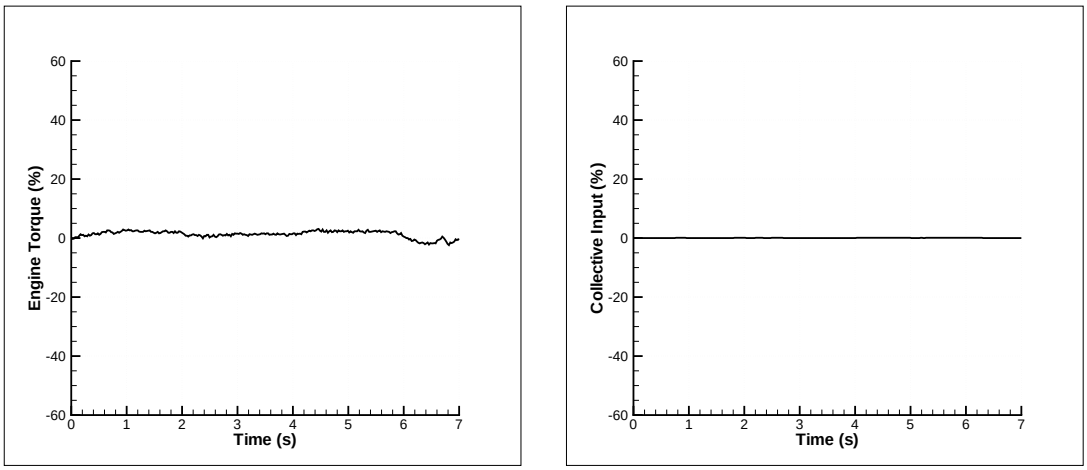

(a) (b)

Figure 5.30: Engine Torque Change and Pilot Collective Input in Case 6.

(a) Engine Torque (b) Pilot Collective Input

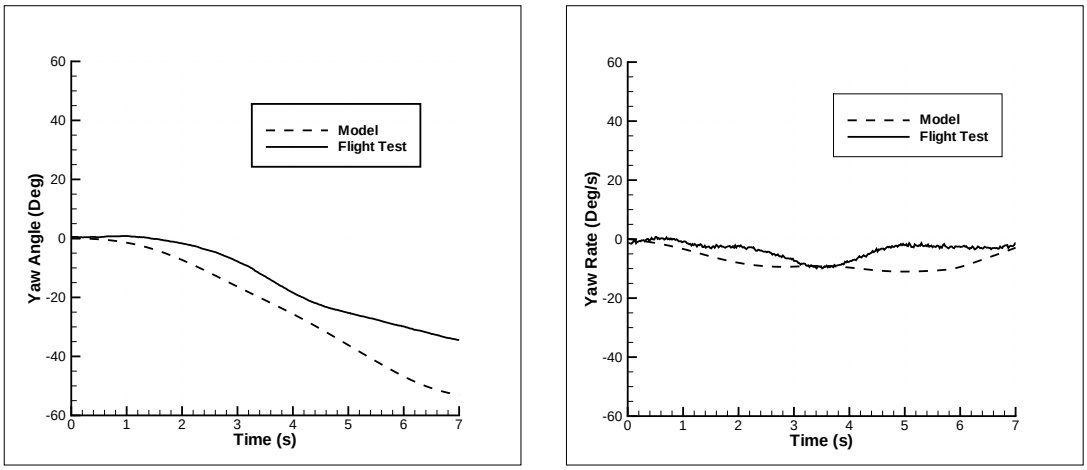

(a) (b)

Figure 5.31: Yaw Axis Response Comparison to the Pilot Pedal Input in Case 6.

(a) Yaw Angle Response Comparison (b) Yaw Rate Response Comparison

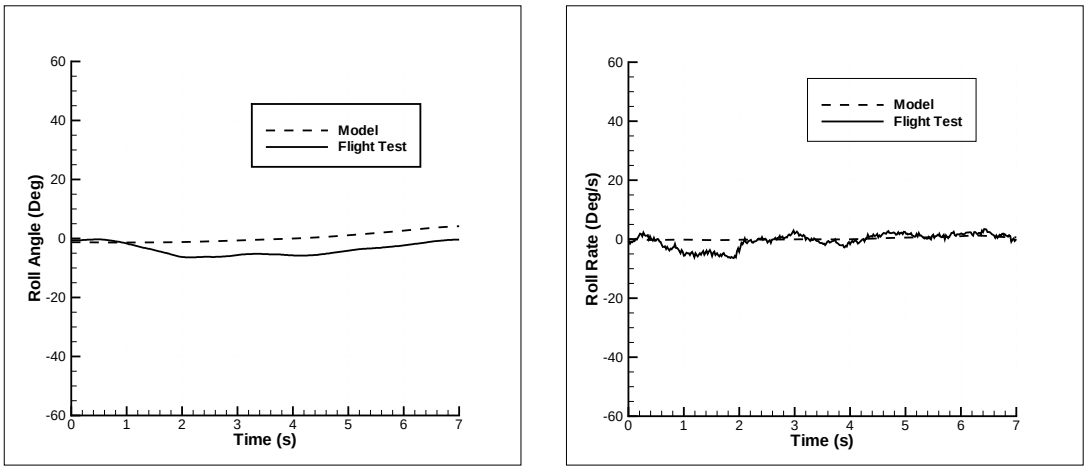

(a) (b)

Figure 5.32: Roll Axis Response Comparison to the Pilot Pedal Input in Case 6.

(a) Roll Angle Response Comparison (b) Roll Rate Response Comparison

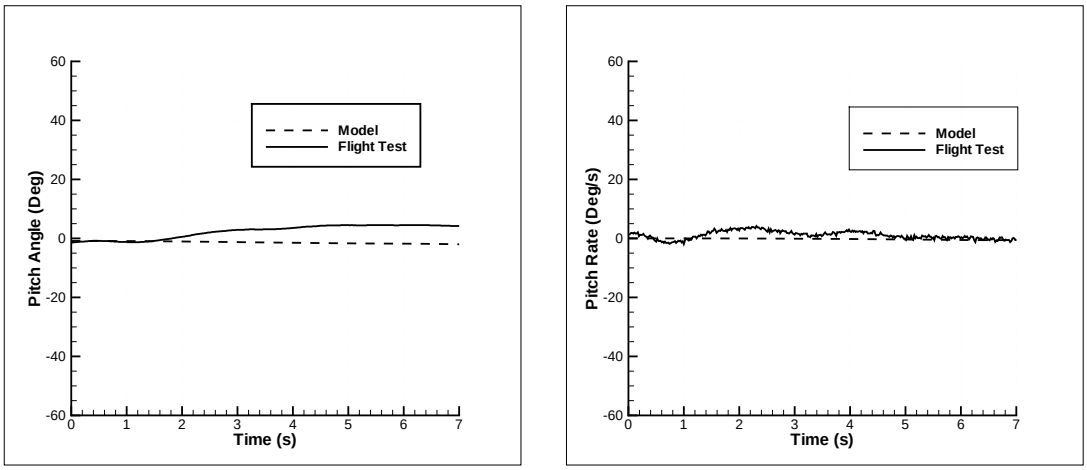

(a) (b)

Figure 5.33: Pitch Axis Response Comparison to the Pilot Pedal Input in Case 6.
(a) Pitch Angle Response Comparison (b) Pitch Rate Response Comparison

This case is the 60 knot forward flight velocity case. In this case the pilot finds the trim position at 60 knot into the wind and applies firstly left pedal and when it reaches to a maximum value, then applies right pedal input. This can be seen from figure 5.29. Again the pilot collective control is nearly perfect and the cyclic input can be assumed to be zero.

In fact, during forward flight most of the anti torque is produced by the vertical tail. Circulation control tail boom provides less than quarter of the anti-torque. Therefore when pedal input is applied the direct thruster exit area and vertical tail incidence angle changes and this causes a change in the anti-torque value. From the figure 5.31 it can be seen that the yaw axis response is close to the flight test. Considering the forces created by the fuselage are also effective on forward flights, most of the error is predicted to be resulted due to the simplified fuselage model.

Figures 5.33 and 5.32 show the pitch and roll axis responses.

5.9 Case 7

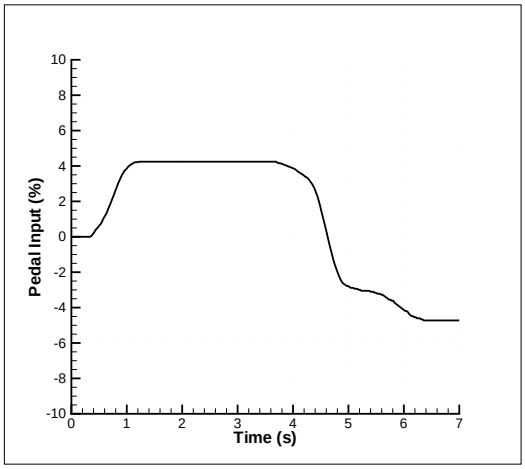

Figure 5.34: Pilot Pedal Input in Case 7

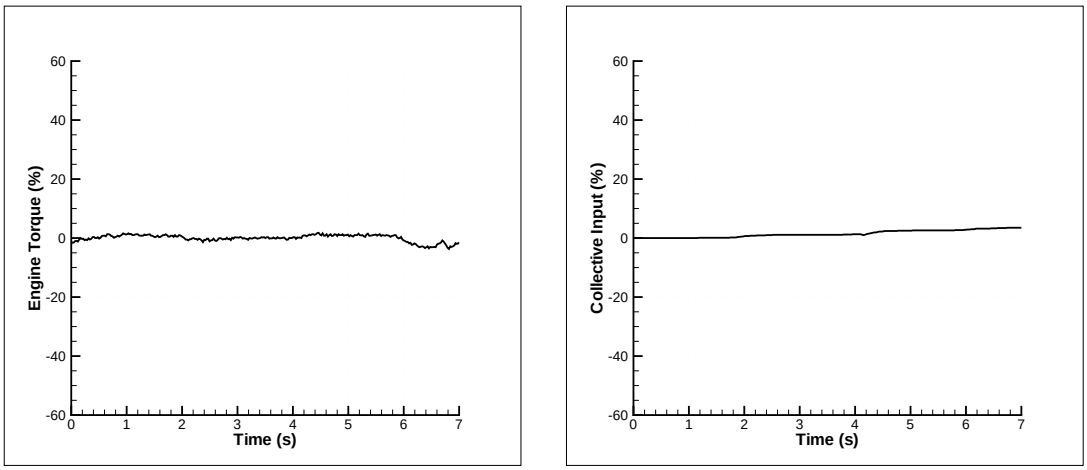

(a) (b)

Figure 5.35: Engine Torque Change and Pilot Collective Input in Case 7.

(a) Engine Torque (b) Pilot Collective Input

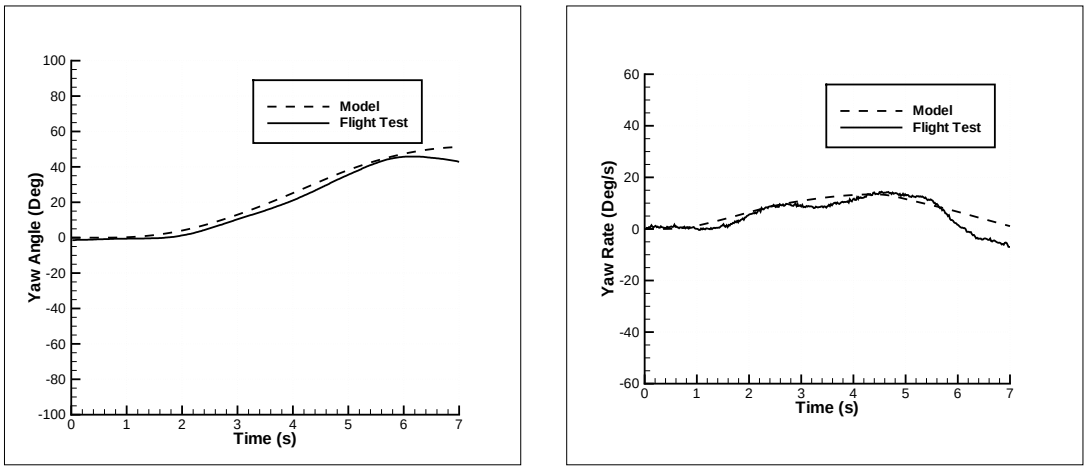

(a) (b)

Figure 5.36: Yaw Axis Response Comparison to the Pilot Pedal Input in Case 7.

(a) Yaw Angle Response Comparison (b) Yaw Rate Response Comparison

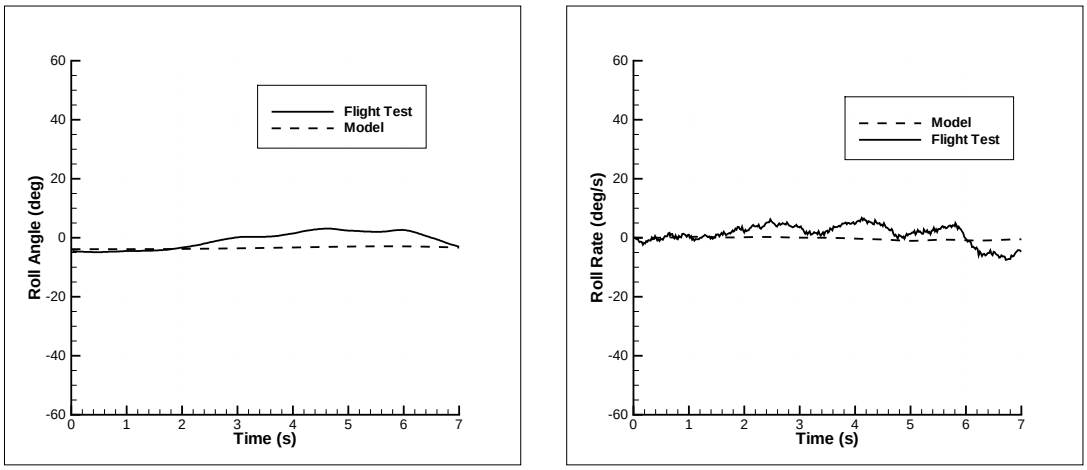

(a) (b)

Figure 5.37: Roll Axis Response Comparison to the Pilot Pedal Input in Case 7.

(a) Roll Angle Response Comparison (b) Roll Rate Response Comparison

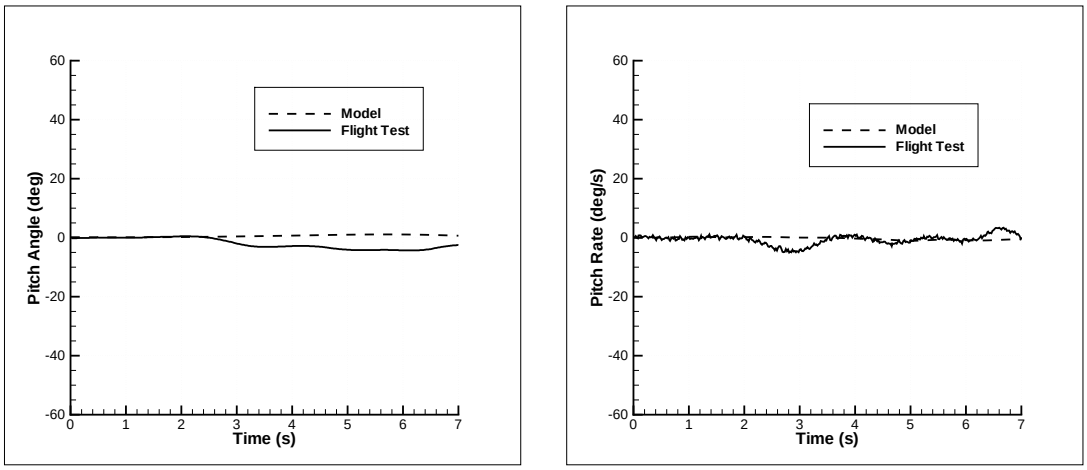

(a) (b)

Figure 5.38: Pitch Axis Response Comparison to the Pilot Pedal Input in Case 7.
(a) Pitch Angle Response Comparison (b) Pitch Rate Response Comparison

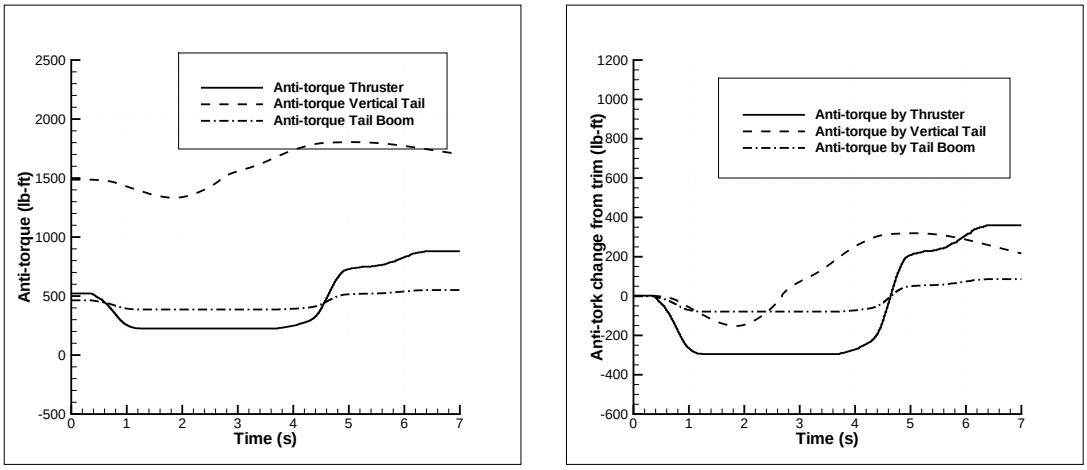

(a) (b)

Figure 5.39: Anti-torque Response to the Pilot Pedal Input in Case 7.
(a) Anti-torque Production (b) Anti-torqu Production Change from Trim

In this case the pilot applies a right pedal at first and keeps it for a while and then applies left pedal. Again the pilot collective control is nearly perfect and the cyclic input can be assumed zero.

Regarding the figure 5.36 it can be seen that there is a nearly perfect match between the model response and the flight test response. Due to the aerodynamic condition of the forward flight, it is known that most of the anti-torque is produced by the vertical tail during forward flight and this can be seen from 5.39a. On the other side thruster is also effective in controls, which

can be seen from 5.39b. Therefore, the reason of the perfect match is the model of thruster and vertical tail.

Looking to all graphs in all cases (figures between 5.1 and 5.38), although the similarity of the results implies the adequate NOTAR model approach for a simulation, it can be seen that the match is not perfect.

The following could have caused a mismatch between the simulation model and flight tests ;

- the assumptions that are made in simplified mathematical model, especially in modeling the flow over the tail boom,
- the wind effect which could not be modeled well,
- the assumptions made in the properties of the helicopter,
- the errors in minimum complexity theory.

Other flight test related errors are as follows;

- pilot errors during the flight test,
- wind can not be measured well,
- the errors of the test instruments.

Although the model responses are not perfectly matched with the flight test responses, the results imply that it is an adequate model approach for a simulation and it shows that the developed model is a valid model of a NOTAR system.

CHAPTER 6

CONCLUSION

In this study, a mathematical model of an anti-torque system of a NOTAR helicopter is developed. The model is integrated into a simulation program which is based on the minimum complexity models. In addition, flight tests are performed on the MD 600N NOTAR helicopter to verify the results. Then simulation results are compared with the ones obtained from flight tests.

Since the anti-torque production of each element varies with flight regime, the flight characteristics of the traditional tail rotor and NOTAR is not the same. Therefore completely different model is developed in this thesis. The developed model is not only based on aerodynamic calculations but also flight test results. During the model development two main assumptions are made referring to the results of the studies. The first assumption is that the circulation control tail boom which produces 60% of the anti-torque in hover trim condition. The second assumption is fan maintains internal boom pressure by changing mass flow rate that keeps exit velocity from the thruster constant. By the model developed based on these two assumptions, internal boom pressure which is constant and has a value between 0.5 to 1 psi above the outside air pressure is obtained.

The developed model is integrated to a program baseline of the minimum complexity theory [12]. MD 600N helicopter properties are included to the program. Some modification on the program is made while integrating NOTAR model and the helicopter properties into the simulation program and some unknown information about helicopter is evaluated by measuring the shapes and comparing with the similar helicopters.

Analyzing the model it is observed that there is a close relationship between the direct jet

thruster exit area and pitch angles of the NOTAR fan blades. When the thruster exit area changes, fan blade pitch angles also change in a manner to differ the flow rate which keeps the angle of attack on the fan blades constant. Although this does not provide constant fan pressure ratio, the air pressure becomes constant value when it achieves to the boom passing through stators and diffuser.

A flight test on MD 600N helicopter is accomplished in order to verify the model. Seven of them are selected for comparison. Then the flight test data is compared with the model data which is acquired by applying the same inputs as the pilot has done during the test flight. The results showed that model responses are close to the real helicopter responses. The yaw axis responses of the model are in reasonable levels. But model right pedal responses are slower than the real flight right pedal responses. This is an expected situation because the developed NOTAR model has symmetrical responses as many tail rotor models. The difference between the flight test and the model responses are mostly caused by the wind which could not be modeled good enough in simulation.

During flight test it is seen that the boom torque response is effected by side winds. Therefore, NOTAR helicopter pilots should be careful on high wind air conditions during hover and low speed flights, where the boom is needed to be effective. If it is a high wind speed condition then it is safer to take off and land into the wind.

The NOTAR model performed well in the real-time simulation and presented satisfactory handling qualities in the yaw axis. When compared to the flight tests, the yaw axis response was satisfactory, but the off-axis responses where sometimes somewhat degraded, believed to be mostly due to the lack of modelling of the minimum complexity math model. Yet the model can be used in real-time simulation models.

6.1 Suggested Future Work

This study can be extended with the following items suggested for the future work:

- Better approaches other than minimum complexity model can be used to integrate the NOTAR model
- Better inflow models can be used for the Main Rotor

- Anti-torque production calculations of Circulation Control Tail Boom can be based on more detailed aerodynamic solutions,
- More detailed NOTAR fan solutions can be found,
- The air momentum ejecting from the thruster can be found more precisely,
- More precise flight test can be obtained (tests on a less windy day),
- More precise properties of the helicopter can be obtained (especially the helicopter inertias),
- More detailed engine parameters can be obtained,
- A detailed wind and turbulence gust model can be implemented to the simulation model.

REFERENCES

[1] E. P. Sampatacosa, K. M. Morger, A.H. Logan "*The Viable Alternative to a Tail Rotor*", Hughes Helicopters, Inc., Culver City, California, 1993

[2] NOTAR History and Development "*http://home.wanadoo.nl/helicopter/development.htm*", as accurate of August 2008.

[3] "*MD 600N Pilot Transition Training Manual*", MD Helicopters Inc., June 2005

[4] P. M. Lambermont, A Pirie "*Helicopters and Autogyros of the World*", Littlehampton Book Services (LBS), 1970

[5] T. Wilcock, C. A. Thrope "*Flight simulation of a Wessex helicopter,a validation exercise* ",Aeronautical Research Council C.P. No. 1299, Aerodynamics Department, R.A.E., Bedford, 1974

[6] S. Dawson, T. Thompson "*Recent NOTAR Anti-Torque System Research and Testing at MDHC*", 49th Annual Forum of the American Helicopter Society, St. Louis, Missouri, May 1993

[7] R. E. Bregger, S. Dawson "*Side-by-side Hover Performance Comparison of MDHC 500 NOTAR and Tail Rotor Anti-torque Systems* ", The 48th Annual Forum of the American Helicopter Society, Washington, June 1992

[8] J. R. VanHorn "*Circulation Control Slots in Helicopter Yaw Control System*", United States Patent Office, May, 1988

[9] D. T. Fisher "*Wind Tunnel Performance Comparative Test Results of a Circular Cylinder and 50 Percent Ellipse Tailboom for Circulation Control Anti-torque Applications*", Master's Thesis, Naval Postgraduate School, Monterey, California, March, 1994

[10] H. Stephena "*NOTAR Proof of Concept*", 1986 Report to the Aerospace Profession, Proceedings of the Thirtieth Symposium, Beverly Hills, CA, September, 1986

[11] R. K. Hefley, M. A. Mnich "*Minimum-Complexity Helicopter Simulation Math Model*", Contract NAS2-11665, Muadyne Report 83-2-3, Ames Research Center , October 1986

[12] D. Yılmaz "*Evaluation Comparison of Helicopter Simulation Model with Different Fidelities*", Master's Thesis, Middle East Technical University, Aerospace Engineering Department, Ankara, July, 2008

[13] J. G. Lee "*Helicopter Anti-torque Device*", United States Patent Office, October 1992

[14] A. H. Logan, R. P. Verdes, R. E. Moore "*Helicopter Anti-torque System Using Circulation Control* ", United States Patent Office, December, 1977

[15] K. M. Morger, D.R. Clark "*Analytic and Experimental Verification of the NOTAR Circulation Tail Boom*", The 40th Annual Forum of the American Helicopter Society, Arlington, VA, May, 1984

[16] K. Saripalli "*Ground Test of Hovering V/Stol Aircraft and NOTAR helicopters in the Hover Research Faacility at McDonnell Douglas Aerospace* ", 33rd Aerospace Sciences Meeting and Exibit, Reno, NV, January, 1995

[17] "*MD 900N Technical Description*", MD Helicopters Inc, Mesa, Arizona, January, 2001

[18] "*MD 600N Technical Description*", MD Helicopters Inc, Mesa, Arizona, January, 2001

[19] "*MD 500N Technical Description*",MD Helicopters Inc, Mesa, Arizona, January, 2001

[20] R. A. Wallis "*Axial Flow Fans and Ducts*", Wiley-Interscience Publication, 1983

[21] J. D. Anderson "*Fundamentals of Aerodynamics*", McGraw-Hill International Editions,1991

[22] J. L. Kerrebrock "*Aircraft Engines and Gas Turbines*", The MIT Press, Cambridge, Massachusetts, 1992

[23] J. G. Leishman "*Principles of Helicopter Aerodynamics*", Cambridge University Press, 2006

[24] J. L. Valezquez "*Anti-torque Propulsion and Directional Control System*", United States Patent Office, November, 1972

[25] M. Olmstead, E. Brown, B. Stringer, J. Masters, J. Johnson, Y. Li "*Pegasus Personal Air Vehicle, The future in personal travel*", Georgia Institute of Technology, Atlanta, Georgia, July, 2002

[26] P. D. Talbot, L. D. Corliss, "*A Mathematical Force and Moment of a UH-1H Helicopter For Flight Dynamics Simulations*", NASA TM 73-254, June 1977

Appendix A

MD 600N SPECIFICATIONS

A.1 MD 600N Dimensions

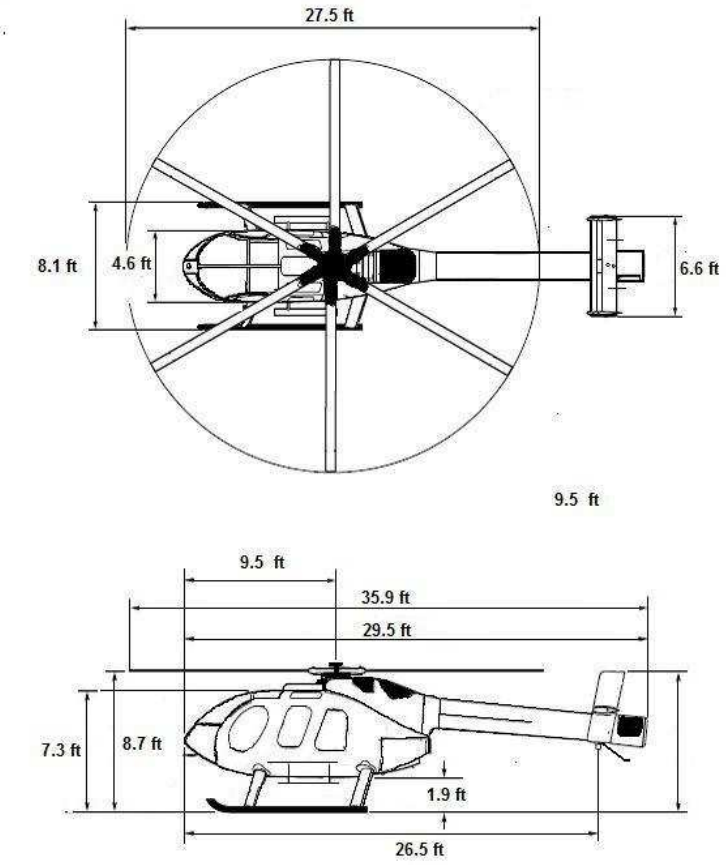

Figure A.1: Dimensions of MD 600N [18]

A.2 MD 600N Performance Specifications

MD600N Performance Specifications 3,600 lb

Maximum Cruise Speed	KTAS Sea Level Standard 5,000 ft, ISA	139 143
Maximum Permitted Speed	Vne (KCAS) at Sea Level	152 (175)
Maximum Range	Sea Level 5,000 ft, ISA	357 (411) 401 (461)
Maximum Endurance	Sea Level 5,000 ft, ISA	3.8 4.1
Maximum Rate-of-Climb	Sea Level Standard ISA + 20 °C Day	1,700 1,500
Maximum Operating Altitude Service Ceiling	Density Altitude ISA @ 100 ft/min	20,000 18,500
Hover In-Ground Effect (HIGE)	Standard Day ISA + 20 °C Day	14,500+ 11,600
Hover In-Ground Effect (HIGE)	Standard Day ISA + 20 °C	11,700 8,000
Certification Limits:		
Standard Weight	Normal Category External Load Empty	4,100 lb 4,700 lb
Empty Weight	Standard Configuration Industrial Configuration	2,100 lb 2,036 lb
Useful Load	Internal External	2,000 lb 2,600 lb
Cargo Hook Structural Rating		3,000 lb
Fuel Capacity		115 gal

Powerplant: Rolls-Royce Allison Engine Company Model 250-C47M gas turbine, rated at 603 kw (808 shp), derated for reliability and safety to:
For take off 447 kw (600 shp)
Max Continuous Power 395 kw (530 shp)

Figure A.2: Performance Specifications of MD 600N [18]

Appendix B

FIGURES FOR LOSS CALCULATIONS

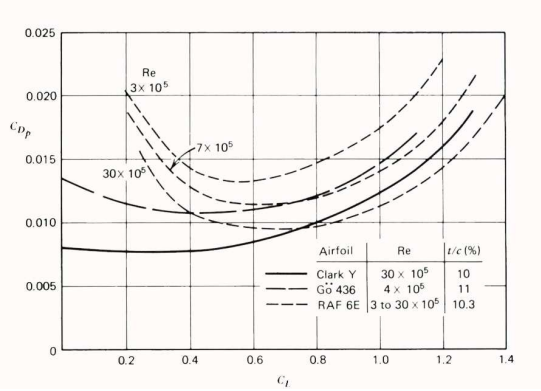

Figure B.1: C_{D_P} versus C_L data for flat undersurface airfoils [20]

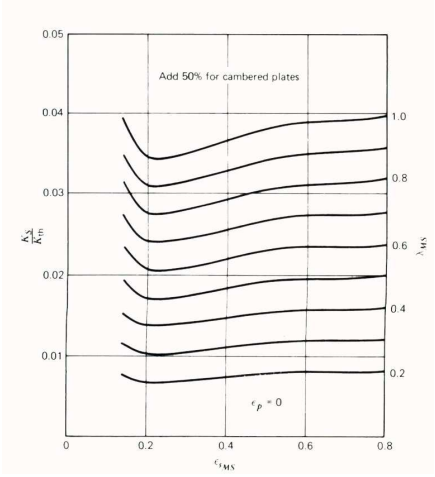

Figure B.2: Straightener efficiency loss for specified designs [20]